Journal Pre-proofs

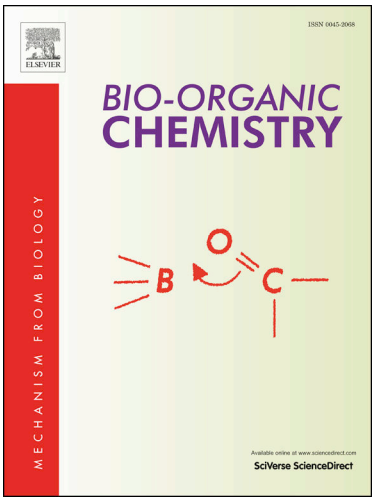

Design and Synthesis of Novel Tranilast Analogs: Docking, Antiproliferative Evaluation and *In-silico* Screening of TGFβR1 Inhibitors

Magda M.F. Ismail, Heba S.A. El-Zahabi, Rabab S. Ibrahim, Ahmed B. M. Mehany

PII: S0045-2068(20)31666-7
DOI: https://doi.org/10.1016/j.bioorg.2020.104368
Reference: YBIOO 104368

To appear in: *Bioorganic Chemistry*

Received Date: 21 April 2020
Revised Date: 22 September 2020
Accepted Date: 8 October 2020

Please cite this article as: M.M.F. Ismail, H.S.A. El-Zahabi, R.S. Ibrahim, A. B. M. Mehany, Design and Synthesis of Novel Tranilast Analogs: Docking, Antiproliferative Evaluation and *In-silico* Screening of TGFβR1 Inhibitors, *Bioorganic Chemistry* (2020), doi: https://doi.org/10.1016/j.bioorg.2020.104368

Design and Synthesis of Novel Tranilast Analogs: Docking, Antiproliferative Evaluation and *In-silico* Screening of TGFβR1 Inhibitors

Magda M.F. Ismail[a]*, Heba S.A. El-Zahabi[a], Rabab S. Ibrahim[a], Ahmed B. M. Mehany[b]

[a]*Department of Pharmaceutical Chemistry, Faculty of Pharmacy (Girls), Al-Azhar University11754, Nasr City, Cairo, Egypt.*

[b]*Department of Zoology, Faculty of Science (Boys), Al-Azhar University11754, Nasr City, Cairo, Egypt.*

ABSTRACT

The discovery of the antiproliferative potential of tranilast prompted additional studies directed at understanding the mechanisms of tranilast action. Its inhibitory effect on cell proliferation depends principally on the capacity of tranilast to interfere with transforming growth factor beta (TGFβR1) signaling. This work summarizes design, synthesis and biological evaluation of sixteen novel tranilast analogs on different tumors such as PC-3, HepG-2 and MCF-7 cell lines. The in vitro cytotoxicity was evaluated using MTT assay showed that, twelve compounds out of sixteen showed higher cytotoxic activities (IC_{50}'s 1.1 -6.29 μM), than that of the reference standard, 5-FU (IC_{50} 7.53 μM). The promising cytotoxic hits ***(4b, 7a, b*** *and* ***14c-e)****, proved to be selective to cancer cells when their cytotoxicity's are examined on human normal cell line (WI-38). Then they are investigated for their possible mode of action as TGFβR1 inhibitors; remarkable inhibition of TGFβR1 by these hits was observed at the range of IC_{50} 0.087 – 3.276 μM. The cell cycle analysis of the most potent TGFβR1 inhibitor****, 4b*** *revealed cell cycle arrest at G_2/M phase on prostate cancer cells. Additionally, it is clearly indicated apoptosis induction at Pre-G1 phase, this is substantiated by significant increase in the expression on the tumor suppressor gene, p53 and up regulation the level of apoptosis mediator, caspase-3. In addition, in silico study was performed for validating the physicochemical and ADME properties which revealed that, all compounds are orally bioavailable with no side effects complying with Lipinski rule. The proposed mode of action can be further explored on the light of molecular modeling simulation of the most potent compounds,* ***4b*** *and* ***14e*** *which were docked into the active sites of TGFβR1 to predict their affinities toward the receptor.*

Keywords:

Synthesis, Anticancer activity, TGFβR1, Caspase-3, p-53, Molecular modeling

Corresponding author
Magda M. F. Ismail
Department of Pharmaceutical Chemistry,
Faculty of Pharmacy (Girls), Al-Azhar University,
Cairo 11754, Egypt
magdaismail@azhar.edu.eg
m.elalfy101@gmail.com

1. INTRODUCTION

Although, our understanding of mechanistic studies that lay behind cancer development and advancement has elevated, cancer is still a significant health alarm in multiple advanced countries [1]. Cancer is a key factor of mortality far and wide; it roughly causes 13% of all deaths every year. [2]On September 2018, WHO advertised that; 9.6 million persons died throughout the world; in-depth, about 1 in 6 deaths is as a result of cancer. [3] There is a critical need for novel diagnostic and treatment options as well as illumination of how cells gain the hallmarks, mandatory to become fully malignant. [1] Transforming growth factor-β (TGF-β) superfamily is a leader in the regulation of a large number of physiological processes from development to pathogenesis including cell proliferation, differentiation and apoptosis. [4-6] Three highly homologous isoforms of TGFβ exist in humans: TGFβ1, TGFβ2 and TGFβ3. [7] The most widely studied target in fighting cancer is the Transforming Growth Factor Receptor type I (TGFβR1), a key player in cell proliferation; differentiation and apoptosis. [8] There are many pharmacological approaches to hinder TGFβR1 signaling, such as monoclonal antibodies, vaccines, antisense oligonucleotides, and small molecule inhibitors. [9] A new series of small-molecule TGFβR1 inhibitors such as galunisertib, [10] SB-505124 [11] and tranilast (Rizaben®) [12] were discovered, (Fig. 1). Such small molecule inhibitors target the catalytic kinase domain of TGFβR1 and bind to the ATP-binding pocket of the receptor to inhibit receptor auto-phosphorylation. This prevents initiation of the signaling cascade, and inhibits the growth and proliferation of the cancer cells. [13] Galunisertib (LY2157299 monohydrate) is an oral small molecule inhibitor of the TGFβR I kinase which particularly has negative impact on the phosphorylation of $SMAD_2$, abrogating activation of TGFB signaling pathway. [14] Besides, galunisertib has antitumor activity in animal models bearing tumors such as breast, colon, lung cancers, and hepatocellular carcinoma, prostate cancer. [14] In 1982, tranilast (N-[3,4-dimethoxycinnamoyl]-anthranilic acid) has been approved in Japan and South Korea as anti-allergic drug for treatment of bronchial asthma [15], with indications for keloids and hypertrophic scar added in 1993. [16] The antitumor properties of tranilast were determined in the end of 1980s; where it was emerged that tranilast displayed an inhibitory effect on TGF-β1 receptor. [16] Inhibitory activity of tranilast has been confirmed on several cell lines of breast, pancreas, liver, prostate, glioma cancer, as well as gastric carcinoma and neurofibroma, [16] Tranilast can also inhibit angiogenesis. [17]

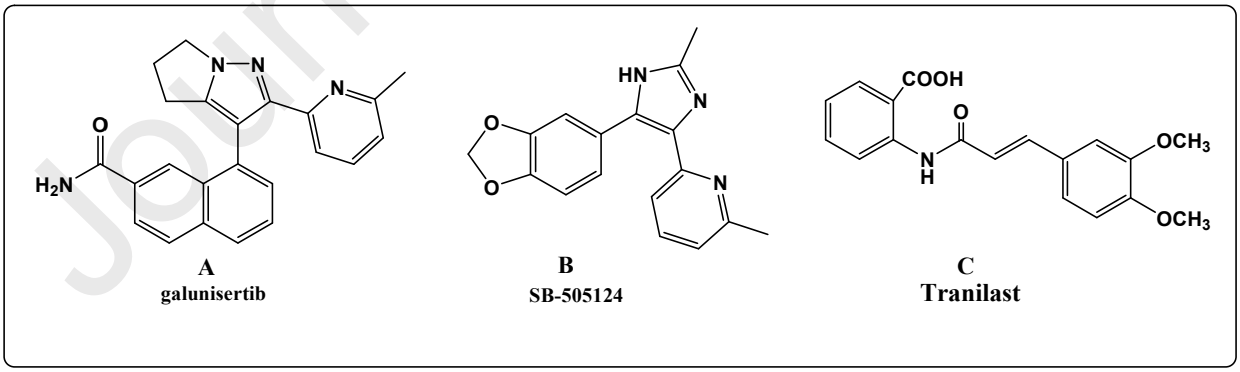

Fig. 1: Structures of small molecules act as TGFBR1 inhibitors

Tranilast was found to decrease the proliferation of fibroblasts from normal tissues and suppress the release of TGF-β from fibroblasts. In addition, its antitumor activity has been reported in some cell lines such as prostate cancer cell lines (PC-3), breast

cancer cell lines like MCF-7, liver, lung and melanoma. Also, Yashiro *et al* [18] have described that, Tranilast decreases the production of MMP-2 and TGF-β1 from fibroblasts, resulting in significant suppression of the invasion ability of gastric cancer cells. It has also been shown to block cell cycle progression, inhibit migration and promote the apoptosis of cells. [19] Several investigations have revealed that, cell cycle arrest is an important mechanism responsible for apoptosis-inducing ability of cancer therapeutic agents in cancer cells. [20] Caspase-3 level and gene expression of p53 were known to be induced in programmed cell death (apoptosis). [20] Structural features of tranilast covered various hydrophilic and hydrophobic points via two terminal modifiable parts; anthranilate and aromatic moieties with central enone modifiable linker, (Fig. 2).

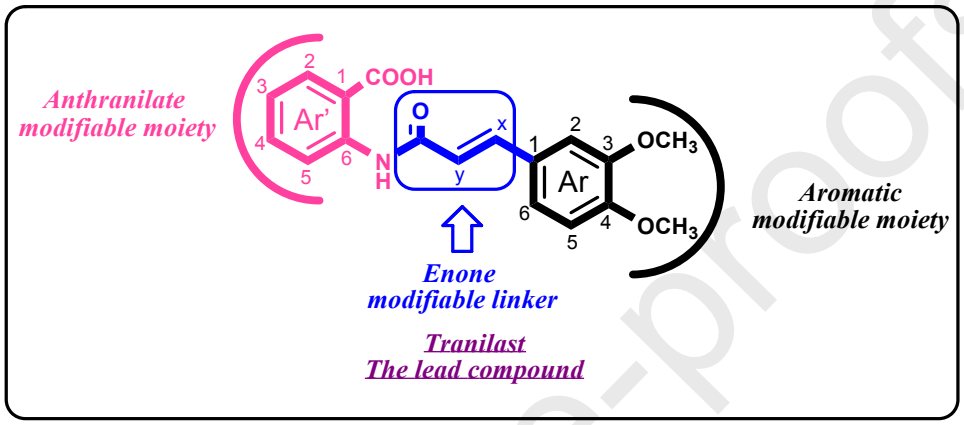

Fig. 2: overview of the modifiable sites of the lead compound Tranilast

Herein, our strategy is directed toward the design and synthesis of four series of tranilast analogs acting as TGFβR1 inhibitors and apoptosis inducers. Concerning series A, ***chain contraction*** strategy was applied where **enaminone linker** is replaced by sulfonamide or amide as in compounds **3a-c** and **4a, b** respectively. Series B, ***bioisosterism*** approach was followed on the **olefinic linker** -CH=CH- which was switched to -CH_2-NH- in N-acetamido analogs, **5a-c**. Series C was designed via ***variation of substituent*** in the **aromatic modifiable moiety** as in chloroacrylamides, **6a-c**, while series D concerned with applying ***ring fusion*** and ***bioisosterism*** strategies on the **anthranilate modifiable moiety** as in acrylamides, **14a-e.** These structural variations were followed in an attempt to optimization of pharmacodynamic and pharmacokinetic properties of tranilast. Additionally, docking of the most potent compounds into human TGF-β using Molsoft ICM 3.4-8c program was performed in order to predict the affinity and orientation of the these compounds to the active site.

2. RESULTS AND DISCUSSION

2.1. Chemistry

Anthranilic acid represents a key starting molecule in many synthetic pathways. N-acetylation of anthranilic acid, **1** using acetic anhydride afforded benzoxazinone intermediate which is immediately hydrolyzed with H_2O to N-acetyl anthranilic acid, **2**. [20-24] N-Sulfonylation [25] of **2** with aryl sulfonyl chlorides in EtOH/TEA/reflux afforded the corresponding sulfonamides **3a-c.** Analogously, benzamide analogs, **4a, b** were prepared using benzoyl chlorides in DMF/reflux, «Scheme 1». Their structures were confirmed by elemental and spectral analysis. IR spectra of compounds **3a-c** demonstrated stretching broad band at the range 2500-3400 cm^{-1} corresponding to OH group and bands at 1670 cm^{-1} and 1710 cm^{-1} for CON and COO groups respectively.^{1}H

NMR spectrum of compound **3a** as an example, revealed a singlet signal at δ 2.13 ppm for $COCH_3$ protons. Two doublets recorded at δ 7.37 ppm and 7.52 ppm disclosed to 4 aromatic protons of *AB* system with ***J*** value 8.00 Hz in addition to 4 aromatic protons of anthranilic moiety. ^{13}C-NMR (DMSO-d_6) of compound **3a** revealed signals at δ 19.3 (CH_3), 138.7(C-SO_2), 142.4 (C-N), 168 (C=O amide) and 169.4 (C=O of COOH) ppm in addition to other signals characterizing each structure. Mass spectrum of **3a** showed peaks at *m/z* 397 [M^+, 1.96%] and 399 [M^{+2}, 1.95%] in (1:1) ratio for Br isotope. On the other hand, IR spectra of compounds **4a, b** showed stretching broad band around 3367 cm^{-1} for OH group and bands at 1670 cm^{-1}, 1700 cm^{-1} and 1710 cm^{-1} for three carbonyl groups.^{1}H NMR spectrum of compound **4a** revealed a singlet signal at δ 2.11 ppm for $COCH_3$ protons and two doublets for aromatic protons appeared at δ 8.05 ppm and 8.10 ppm with ***J*** value 8.00 Hz. ^{13}C-NMR (DMSO-*d6*) δ (ppm) showed signals at δ 20.2 (CH_3), 137.3 (C-N), 166.8 (C-F), 172.1 (CONH) and 172.3 (COOH) (experimental section), «Scheme 1». Chloroacetylation of anthranilic acid, **1** with chloroacetyl chloride under reflux condition in benzene/ piperidine afforded 2-chloroacetamidobenzoic acid, **5.** [26, 27] Knoevenagel condensation [28-34] of the latter with different aldehydes or acetophenones in ethanol/TEA yielded the corresponding 2-chloro-acrylamidobenzoic acids, **6a-c** «Scheme 1». Their structures were assigned based on spectral data. IR spectra showed broad bands at 3251-3400 cm−1 corresponding to OH and NH groups. Also, bands appeared at 1661-1705 cm−1 for two carbonyl groups.^{1}H NMR spectra of **6a-c** exhibited a characteristic singlet signals at the range of δ 7.53and δ 7.81 ppm for the olefinic proton, Cl-C=CH in compounds, **6a** and **6b** respectively. Also, ^{1}H NMR spectrum of **6c** showed a characteristic singlet at δ 2.56 ppm corresponding to the methyl protons (Cl-C=C-CH_3). ^{13}C-NMR (DMSO-*d6*) δ (ppm) displayed signals at δ 11.7 for CH_3, also two signals were observed at 163.8 and 169.4 ppm corresponding to the two carbonyl groups, (experimental section). Mass spectrum of **6c** showed peaks at *m/z*: 349.14 (8.53, M^+) and 351.35 (2.27, M^{+2}) in 3:1 ratio for Cl isotope and base peak at 86.03 (100). Additionally, nucleophilic substitution reaction was performed on compound **5** with different aryl amines in ethanol/TEA [35, 36] to give the corresponding derivatives, **7a-c,** «scheme 1». The structure of target compounds, **7a-c** was proved by elemental and spectral analysis, (see experimental section).

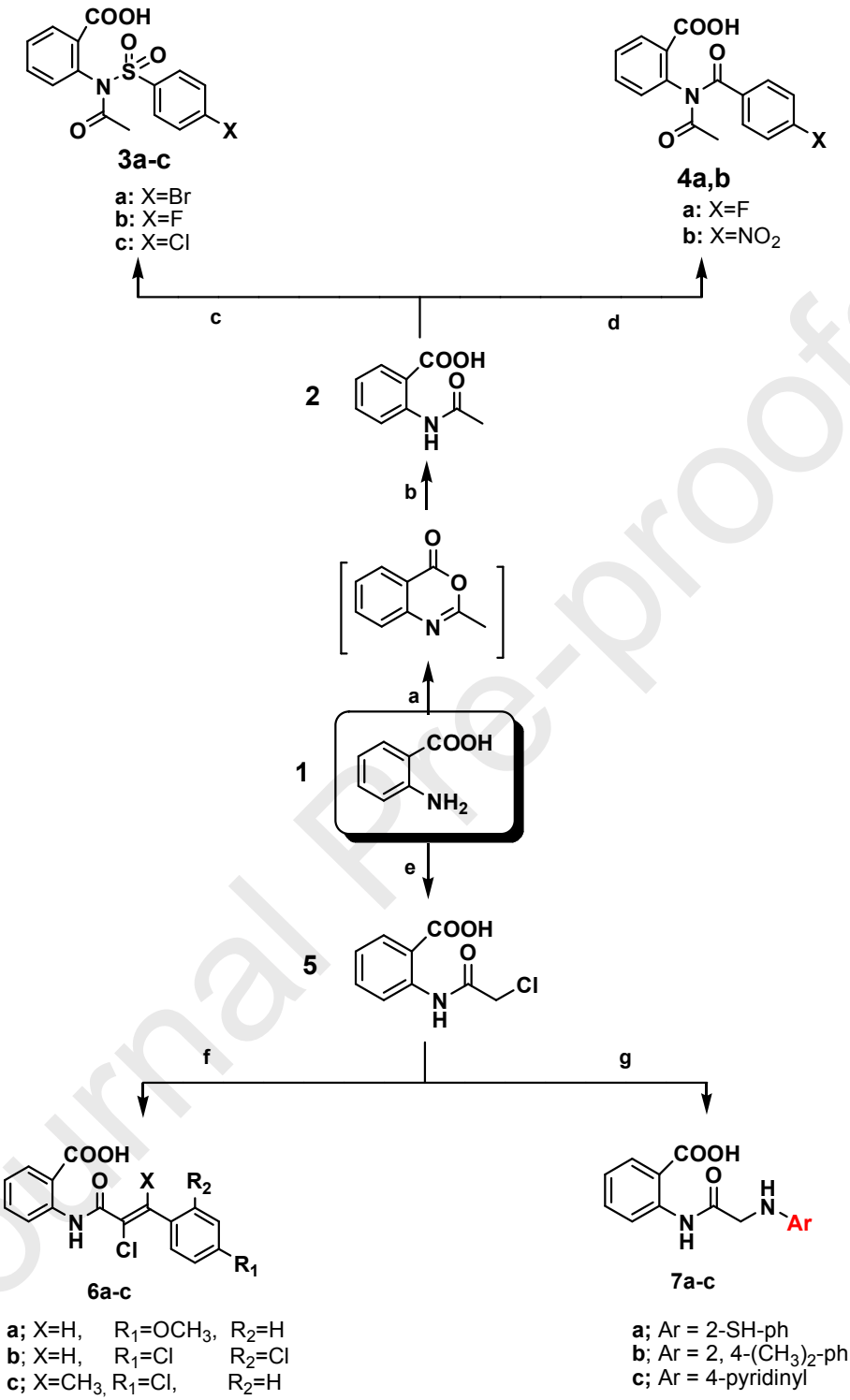

Scheme 1: Reagents and conditions: (a) acetic anhydride, reflux 15 min, cooling; (b) H_2O; (c) *p*-substituted sulfonyl chloride, EtOH, TEA dps, reflux, 5-10 h.; (d) *p*-substituted benzoyl chloride, DMF, reflux, 6-8 h.; (e) $ClCH_2COCl$, benzene, pip., reflux, 6 h.; (f) different aromatic aldehydes and acetophenone, EtOH, TEA, reflux, 8-12 h.; (g) different substituted amines, EtOH, TEA, reflux, 8-12 h.

With the aim of preparing series of tranilast–based analogs bearing various bicyclic systems, nucleophilic substitution reaction of 2-aminothiophene derivatives, **10** with the appropriate cinnamoyl chlorides, **13** in acetone / anhyd. K_2CO_3 /reflux [37] gave the target compounds, **14a-e,** «Scheme 2». The first intermediate, 2-aminothiophene derivatives, **10** were prepared following Gewald reaction [38-43] via reacting equimolar amounts of alicyclic ketones e.g. cyclohexanone, **8a** or cyclopentanone, **8b** with the appropriate active methylene reagent e.g. ethyl cyanoacetate, **9a** or malononitrile, **9b** and elemental sulfur in absolute ethanol / morpholine. [44] The second intermediate, cinnamoyl chloride derivatives, **13** were prepared starting with Knoevenagel condensation [32, 45 and 46] between substituted benzaldehydes, **11** and malonic acid in ethanol/ pip/reflux to produce the corresponding cinnamic acids, **12**. Then; chlorination of **12** using $POCl_3$/ TEA, [47] afforded the corresponding cinnamoyl chloride derivatives, **13**. The IR spectra of **14a-e** showed characteristic stretching bands at 3220 and 2200 and 1650 cm^{-1} corresponding to NH, CN and CO groups respectively.^{1}H NMR spectra of **14a-e** exhibited two characteristic multiplet signals at δ 1.65 ppm and 2.49 ppm corresponding to the protons of cyclohexane. In case of cyclopentane; two multiplet signals appeared around δ 1.95 ppm and 2.5 ppm. Generally, two more doublets appeared at δ 7.25 and 7.96 ppm for olefinic protons CH=CH with *J* constant 16 Hz confirming tran (*E*) configuration (see experimental section).

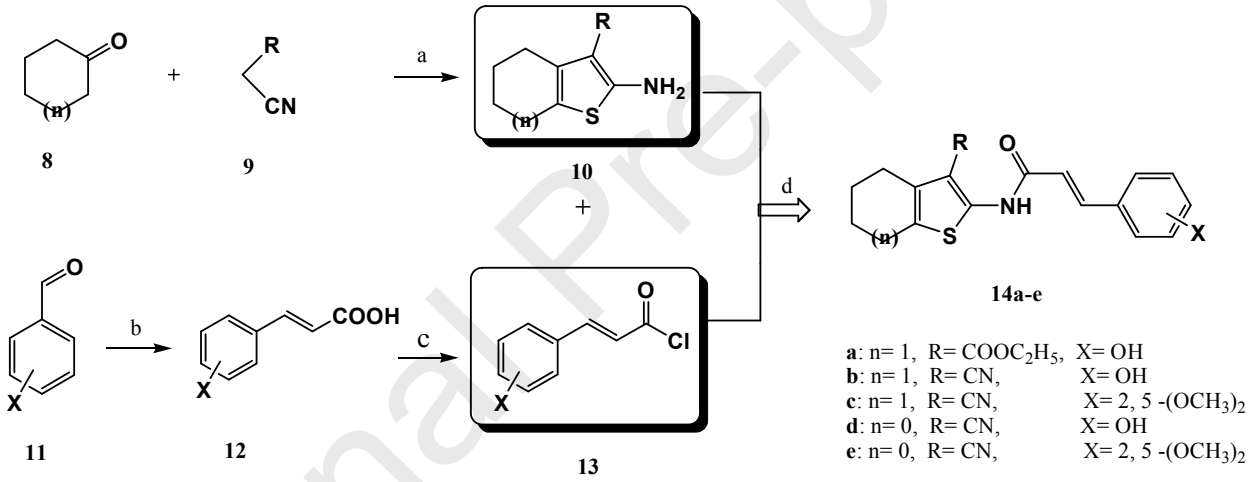

Scheme 2: Reagents and conditions: (a) Elemental sulfur, morpholine , EtOH, reflux 4 h., cooling at 0 ^oC for 24 h; (b) malonic acid, EtOH, piperidine, reflux 5 h.; (c) $POCl_3$, dps TEA, reflux 20 mins; (d) acetone, anhydrous K_2CO_3, reflux, 6-8 h.

2.2. Biological results and discussion

2.2.1. In vitro anti-cancer activities

All the target compounds, **3a-c, 4a, b, 6a-c, 7a-c** and **14a-e** were tested for their anticancer activity using MTT assay [48] against three cancer cell lines e.g. prostate cancer cell **(PC-3)**, hepatocellular carcinoma **(HepG-2)** and human breast adenocarcinoma **(MCF-7)** using 5-FU as a reference standard, **(**Table1). Obviously, the activity pattern of each compound showed correlated results on the three cell lines. Conclusively, prostate cell line (**PC-3**) is the most sensitive one towards our hits.

2.2.1.1 Antiprostate cancer activity (anti PC-3):

The antiproliferative profiles of the test compounds, **3a-c, 4a, b, 6a-c, 7a-c, and 14a-e** showed variable activities compared to the reference standard, 5-FU (IC_{50} 7.53 μM), (Table 1). The highly potent area was covered by benzamido analog **4b**, chloroacrylamido derivative **6b**, acetamido analogs **7a,b** and acrylamides **14c-e** showing IC_{50} values, 1.1, 4.0, 2.7, 3.4, 2.64, 3.4, and 1.35 μM respectively. Compounds **4b** and **14e** were almost equipotent exerting seven folds the activity of 5-FU. Acetamido derivative, **7a** and acrylamide, **14c** were almost equipotent eliciting 2.5 folds the activity of 5-FU. Furthermore, compounds **7b** and **14d** displayed double the cytotoxicity of 5-FU. Another target compounds e.g. **3a-c, 4b** and **14a, b** showed better anticancer activity than 5-FU, their IC_{50s} ranges from 4 - 6.26 μM). The rest of compounds exhibited moderate to poor activity compared to reference standard, (Table 1).

2.2.1.2. Antihepatic cancer activity (anti HepG-2):

The cytotoxicity of the target compounds on HepG-2 cancer cell line was parallel to the results on PC3 cell line. The most potent derivatives were benzamido analog **4b**, chloroacrylamido analog **6b**, acetamido analogs **7a,b** and acrylamides **14c-e** having IC_{50s} 1.5, 4.55, 3.2, 4.25, 2.85, 3.55, and 2.7 μM respectively compared to 5-FU (IC_{50} 8.15 μM). The mentioned analogs showed two to seven folds the activity of 5-FU against HepG-2 cancer cell line. Some derivatives were equipotent or slightly more potent than 5-FU e.g. **3a-c** and **14a, b** and the rest of compounds demonstrated moderate to poor cytotoxicity, **(**Table 1**).**

2.2.1.3. Antibreast cancer activity (anti MCF-7):

The previous competitive test compounds e.g. **4b**, **6b**, **7a, b** and **14c-e** were also the key analogs in fighting MCF-7 cell line. Among them, the benzamido analog, **4b** showed three folds the activity (IC_{50} 2.6 μM) of 5-FU (IC_{50} 7.76 μM). Equipotent acrylamides **14c, e** (IC_{50} 3.5, 3.2 μM) were twice times more active than 5-FU. Concerning **6b**, **7a, b** and **14d,** they disposed 1.5 folds the activity of 5-FU where their IC_{50s} are 4.79, 4.16, 4.85, and 4.92 μM respectively. The rest of the test compounds exhibited moderate to poor activity compared to reference standard, **(**Table 1**).**

Table1
In vitro anti-proliferative activities towards PC-3, HepG2 and MCF7 cell lines.

Compound No.	IC_{50}% (μM) ± S.E.		
	PC-3	HepG-2	MCF-7
3a	**5.11 ± 0.72**	**6.51 ± 0.84**	**7.8 ± 0.87**
3b	**5.94 ± 0.65**	**6.42 ± 0.71**	**8.8 ± 0.96**
3c	**4.75 ± 0.53**	**5.73 ± 0.68**	**8.22 ± 0.97**
4a	**8 ± 0.91**	**9.7 ± 1.02**	**11.28 ± 0.67**
4b	**1.1 ± 0.32**	**1.5 ± 0.52**	**2.6 ± 0.42**
6a	**29 ± 1.2**	**31.42 ± 1.32**	**33.16 ± 1.52**
6b	**4 ± 0.52**	**4.55 ± 0.32**	**4.79 ± 0.19**
6c	**16.45 ± 0.98**	**18.07 ± 1.22**	**23.62 ± 1.52**
7a	**2.7 ± 0.81**	**3.2 ± 0.42**	**4.16 ± 0.56**
7b	**3.4 ± 0.54**	**4.25 ± 0.94**	**4.85 ± 0.62**
7c	**32.9 ± 1.32**	**36.13 ± 1.92**	**38.2 ± 1.72**
14a	**6.29 ± 0.5**	**8.3 ± 0.75**	**8.27 ± 0.76**

14b	**5.2 ± 0.46**	**7.9 ± 0.67**	**7.5 ± 0.8**
14c	**2.64 ± 0.21**	**2.85 ± 0.17**	**3.5 ± 0.26**
14d	**3.4 ± 0.42**	**3.55 ± 0.28**	**4.92 ± 0.31**
14e	**1.35 ± 0.04**	**2.7 ± 0.19**	**3.2 ± 0.28**
5-FU	**7.53 ± 0.57**	**8.15 ± 0.61**	**7.76 ± 0.46**

2.2.1.4. The effect on normal cell line (anti-WI-38):

On the other hand, the safety profile of the promising compounds (**4b, 7a, 7b, 14c- e**) was further investigated via determination of their cytotoxicity on human normal cell line (WI-38), where the recorded data showed high safety margin of them. Their cytotoxic effect against cancer cell lines was several folds higher than that of normal cell line, (Table 2).

Table 2
Cytotoxicity of all compounds against the human non-cancerous cell line WI-38 cell.

Compound No.	**IC_{50} (µM)a WI-38 cell**
4b	**234.43**
7a	**278.81**
7b	**305.98**
14c	**259.90**
14d	**236.30**
14e	**185.20**

2.2.1.5. Structural activity relationships

Structural profile of the target compounds (**3a-c, 4a, b, 6a-c, 7a-c, and 14a-e**) was based on the anticancer lead compound, tranilast, considering three modifiable sites, anthranilate moiety, enone linker and aromatic moiety for tailoring tranilast analogs, (Fig. 2). As previously mentioned, four main series, A-D were planned via drug rational approaches, (Fig.3). Regarding series A (chain contraction), represented by **3a-c** and **4a, b**, benzamido analog **4b**, was the most potent anticancer agent against prostate, hepatic and breast cancer cell lines with IC_{50} 1.1, 1.5 and 2.6 µM respectively. Replacement of *p*-NO_2 by *p*-F as in **4a** dramatically decreased the activity against the tested cell lines; this could be attributed to the important effect of hydrophilic/hydrophobic balance on the activity. Regarding sulfonamide analogs **3a-c**, that illustrated switching between different halogen atoms e.g. Br, F and Cl, the halogen replacement did not greatly affects the anticancer activity. Interestingly, **3b** with $NHSO_2$ group was more potent than **4a** containing NHCO functionality against the three cancer cell lines. Series B (bioisosterism) represented by compounds **7;** It was found that **7a, b** displayed remarkable anticancer activity against tested cell lines. Noticeably, **7a** (Ar= *o*-SHph) provided a slight increase in anticancer activity than its counterpart, **7b** (Ar=*o,p*-$(CH_3)_2$ph). Nevertheless, **7c** (Ar=*p*-pyridyl) showed low the anticancer activity by almost eight folds compared to 5-FU. In case of series C, enhanced cytotoxicity was recorded for **6b** bearing *o, p*-diCl-ph moiety; when replacing it by e-donating group, *p*-OCH_3-ph as in **6a,** cytotoxicity is completely abolished. This anticancer profile reflected the vital role of e-withdrawing effect on the aromatic modifiable moiety of compounds **6a-c**, **(**Fig. 3**).**

In regard of series D (bioisosterism / ring fusion) included acrylamide derivatives, **14a-e**, potential anticancer activity was exhibited especially for compounds **14c-e**. Generally, replacement of cyclohexan[*b*]thiophene moiety in **14b, c** by cyclopenta[*b*]thiophene moiety in **14d, e**, enhanced the anticancer activity against the tested cell lines. Comparison of the anticancer activity of cyclohexan[*b*]thiophene pairs **14b, c** and cyclopenta[*b*]thiophene pairs **14d, e** reflected the positive impact of 2, 5-$(OCH_3)_2$ groups in **14 c, e** on the anticancer activity rather than 4-OH group in their counterparts **14b, d**, **(**Fig. 3**).** As well, 3-CN group in **14b** showed higher cytotoxicity than 3-ester functionality in **14a**. Collectively, cyclopenta[*b*]thiophene moiety, 3-CN group and 2, 5-$(OCH_3)_2$ are preferred for anticancer activity of acrylamides.

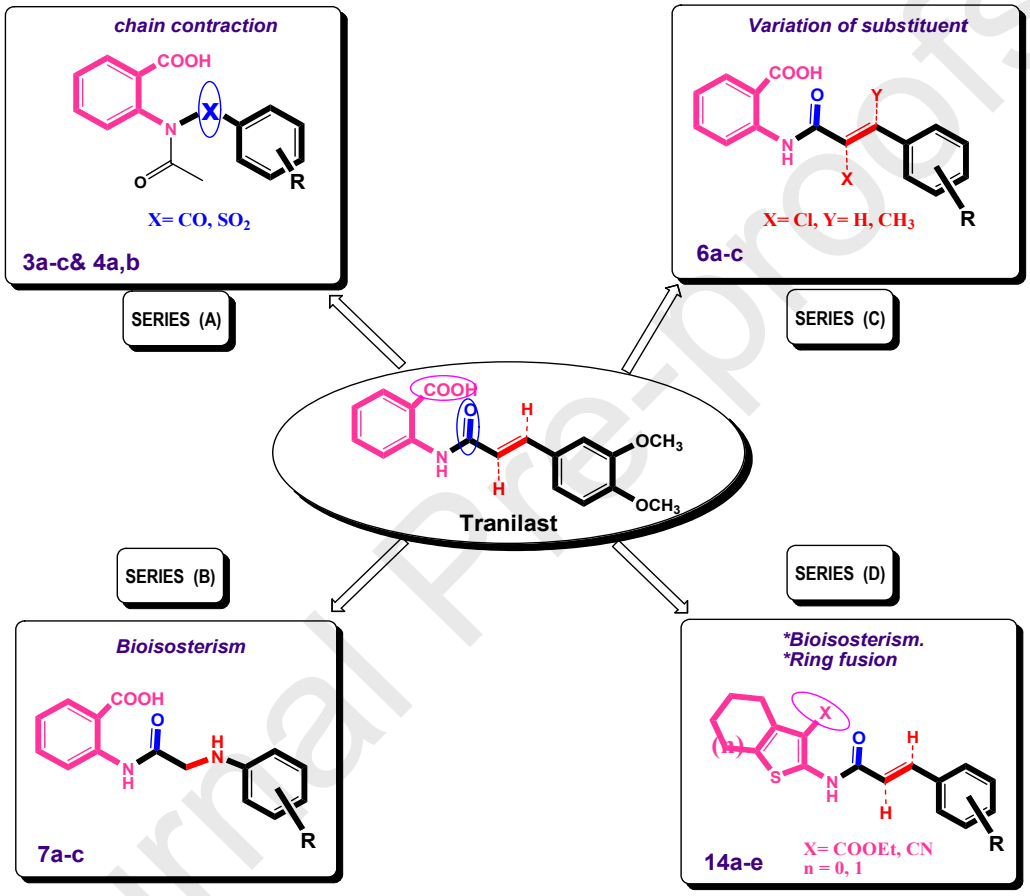

Fig. 3: Design of target compounds as tranilast analogs

2.2.3. TGFBR1 inhibition assay

The most potent hits **4b, 7a,b and 14c-e** (IC_{50} 0.087- 3.276 µM) were selected to explore their mechanism of action; through evaluation of their inhibitory effect against TGFβR1. Results of TGFβR1 assay revealed that compounds **4b**, **7a** and **14e** were the most potent TGFβR1 inhibitors showing IC_{50s} in sub-micromolar range (IC_{50}s 0.08 , 0.09, and 0.19 µM) respectively. Compounds **4b** and **14e** are more potent TGFβR1 inhibitors than the reference standard galunisertib (IC_{50} 0.17µM), while **7a** revealed equipotent inhibition to it, (Table 3).

Table 3
IC_{50} of the representative anticancer active compounds on TGFβR1 in PC-3 cells

Compound No.	IC_{50} (µM) a TGFβR1
4b	0.087 ± 0.064
7a	0.191 ± 0.013
7b	3.276 ± 0.097
14c	1.379 ± 1.42
14d	2.114 ± 0.41
14e	0.093 ± 0.16
Galunisertib	0.170 ± 0.057

2.2.4. Cell cycle analysis

Cell cycle analysis of the most potent antiproliferative TGFβR1 inhibitor **(4b)** was examined [49] to clarify its possible apoptotic inducing effect. Amongst the tested cancer cell lines, PC-3 exhibited the highest sensitivity towards **4b** (IC_{50}=1.1µM). It was obvious from cell cycle analysis on PC-3 that, **4b** induced a significant increase in the percentage of cells at Pre-G1phase by almost 12 folds and increased G2/M by 4 folds, compared to the control experiment, (Table 4). Such increase was accompanied by a decrease in the percentage of cells at the G^o/G1 and S-phases of the cell cycle. The Pre-G1 and G2/M phase results clearly indicated that, compound **4b** induces apoptosis at Pre-G1 phase and arrest the cell cycle at G2/M phase, (Figs. 4a-c).

Table 4
Results of cell cycle analysis in PC-3 cells expressed by (%) of cells in each phase when treated with compound **4b**

Compound No.	%G0-G1	%S	%G2-M	%Pre-G1
4b / PC-3	26.36	15.43	42.37	15.84
Control/ PC-3	56.39	32.44	9.86	1.31

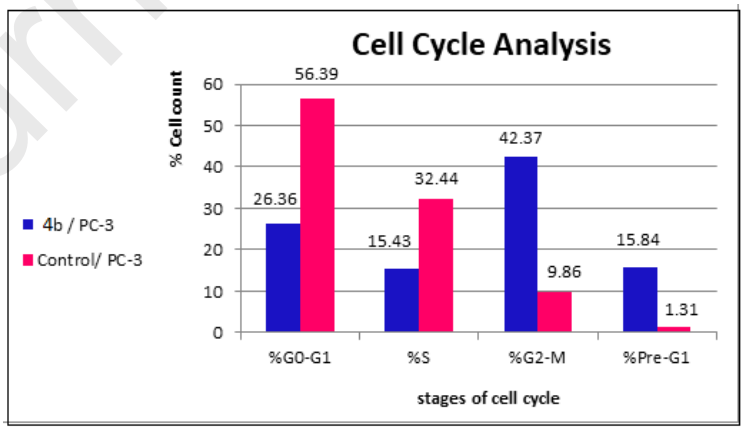

Fig. 4a: Cell cycle analysis and apoptosis effect in PC-3 cell line treated with compounds **4b**

Fig. 4b: Cell cycle analysis of PC-3 cells treated with **DMSO**

Fig. 4c: Cell cycle analysis of PC-3 cells treated with compound **4b**

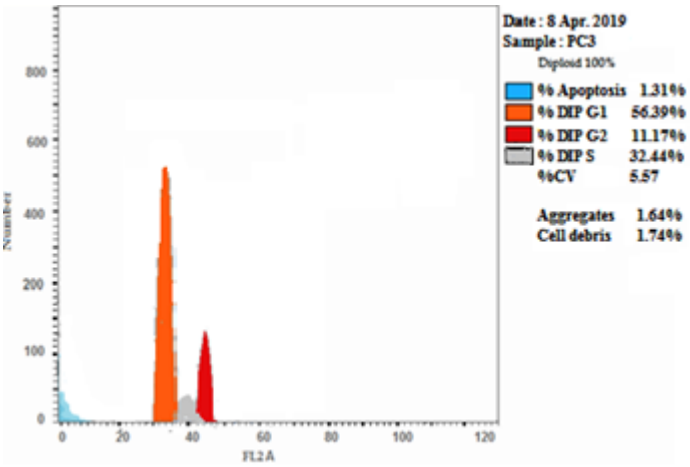

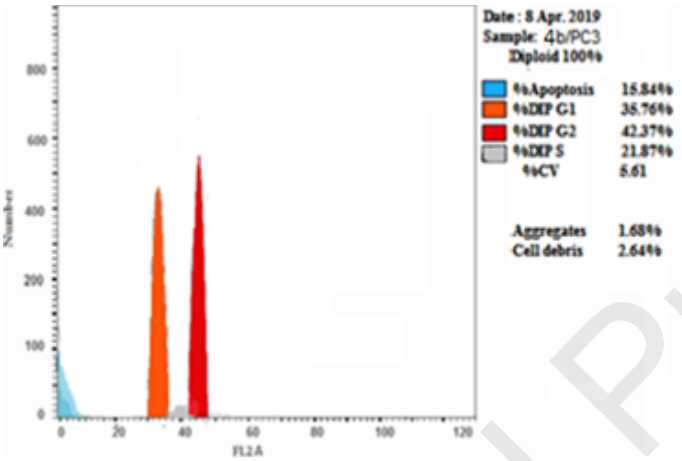

2.2.5. Apoptosis detection studies

2.2.5.1. Annexin V-FITC apoptosis assay

In order to confirm the apoptosis induction of **4b**, Annexin V binding studies by flow cytometer was carried out. [50] As TGFBR1 inhibitors can induce cancer cell apoptosis, the apoptotic inducing effect of compound **4b** against PC-3 cells was evaluated via flow cytometer detection using Annexin V-FITC and propidium iodide (PI) double staining. The results revealed that, compound **4b** increased the early apoptosis ratio (lower right quadrant of the cytogram) from 0.63 to 6.69, and increased the late apoptosis ratio (higher right quadrant of the cytogram) from 0.46 to 6.22 compared to the control experiment, (Table 5). Comparative study for apoptosis illustrated high apoptotic effect of the target compound **4b**; it was 12 folds as much as the control experiment. These data suggest that, compound **4b** triggered apoptosis via the programed cell death pathway rather than necrotic pathway, (Figs. 5a-c).

Table 5
Percent of cell death induced by compound 4b on PC-3 cell.

Compound No.	Total	Apoptosis %		Necrosis %
		Early	Late	

4b / PC-3	15.84	6.69	6.22	2.93
Control/ PC-3	1.31	0.63	0.46	0.22

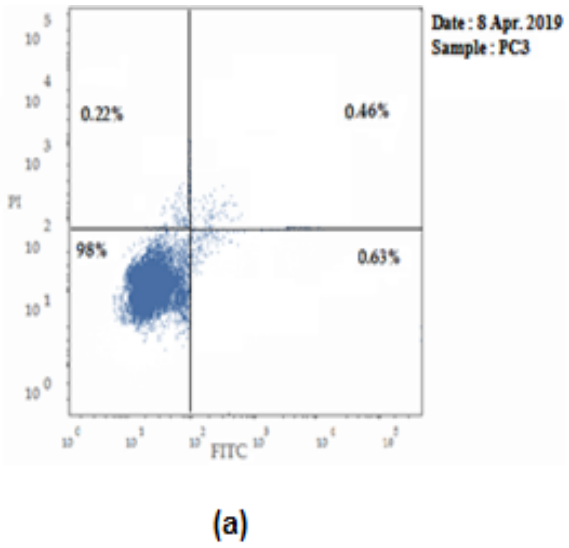

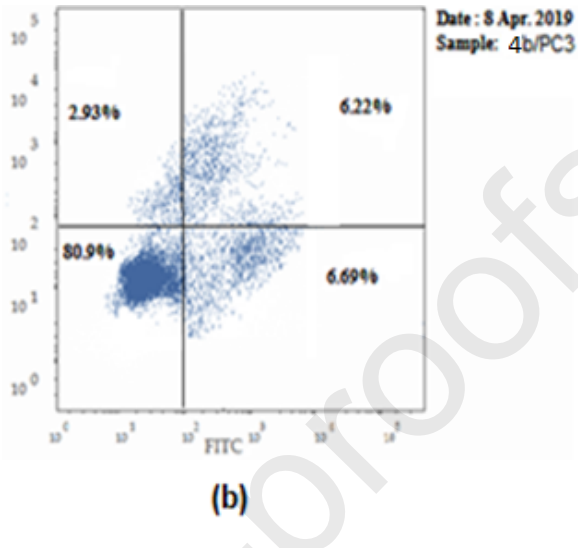

Fig. 5a: Effect of **control** on apoptosis of PC-3 cells

Fig. 5b: Effect of **4b** on apoptosis of PC-3 cells.

The quadrants in the cytograms represent the following: **Necrotic cells** (higher left quadrant of the cytogram); **late apoptotic cells** (higher right quadrant of the cytogram); **Non-apoptotic and non-necrotic cells** (living cells) (lower left quadrant of the cytogram); **early apoptotic cells** (lower right quadrant of the cytogram).

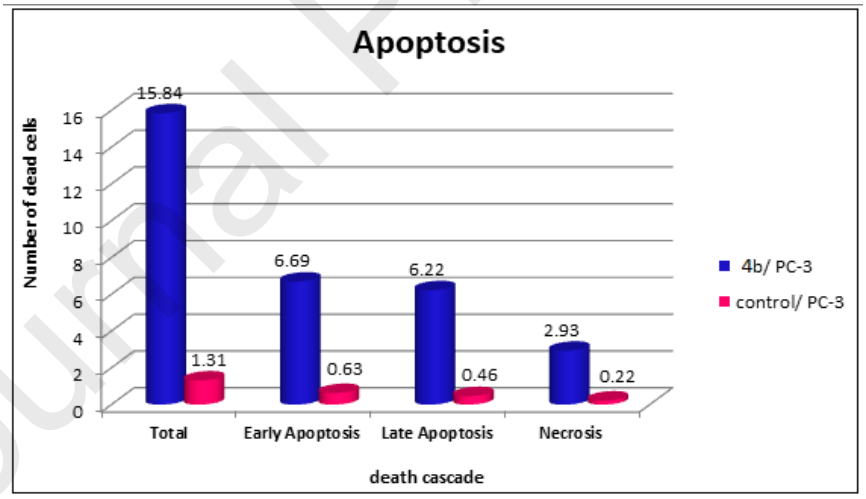

Fig. 5c: Percent of cell death induced by compound **4b** on PC-3 cells.

Fig. 5: Cell cycle analysis; a)-control PC-3, b) compound **4b** by flow cytometer using PI staining method, c)% cell death induced by **4b**

2.2.5.2. Effect on the level of active caspase-3

Activation of the caspase-3 pathway is a hallmark of apoptosis and can be used in cellular assays to quantify activators and inhibitors of the "death cascade." [51] The most active analog, **4b** was evaluated for its effect on caspase-3 and the results revealed

that, **4b** up regulated the caspase-3 level by almost 7 folds compared to the control, (Table 6). So, the recorded data proved the apoptosis induction potential of this target compound, (Fig. 6).

2.2.5.3. Effect on the expression of p53 gene

P53 is the master guardian of the genome which mutated in over 50% of human cancers; its activity stops the formation of tumors. The p53 protein is the product of p53 gene which acts as a regulator of transcription and mediates several biological effects, such as growth arrest and apoptosis. It is believed that, tumor suppressor gene, p53 has the ability to induce apoptosis and growth arrest may be as a result of its role in mastering the expression of a variety of target promoters such as p21, Bax, bcl-2, CDK2 and PUMA α. [52] Results revealed that, **4b** significantly increased the expression of p53 on PC-3 cells by almost 14 times compared to the control and strongly shifted PC-3 cancer cells towards apoptosis, (Table 6, Fig. 6).

Table 6
The effect of compound 4b on the level of caspase-3 and gene expression of p53 gene.

	Conc. (Pg./ml)	
Compound No.	**Caspase -3**	**p53**
4b	362.8	259.6
Control	51.39	19.22

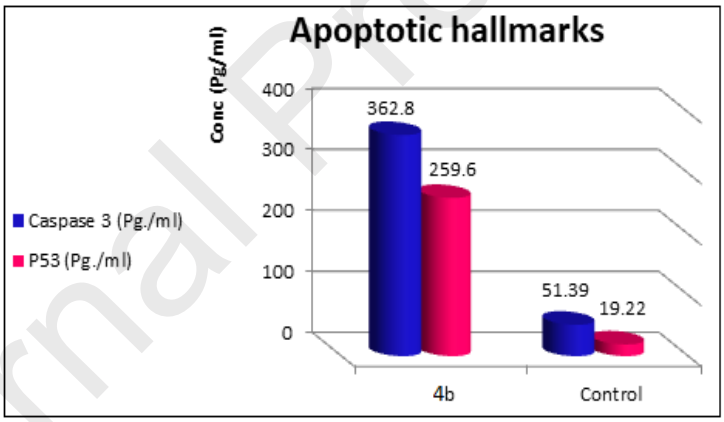

Fig. 6: The effect of **4b** on the level of caspase-3 and p53.

2.3. Molecular Modeling

2.3.1. In-silico evaluation of physicochemical and ADME properties

Computational study of the synthesized compounds was performed to evaluate the physicochemical and ADME properties. SwissADME [53] software was used to predict whether the compounds are likely to be bioactive according to some critical parameters such as Lipinski and Veber rules. As delineated from Table 7; the physicochemical properties of all test compounds have zero Lipinski's violation. Also, all are in agreement with the parameters of veber rule [54], this indicates that these derivatives have promising drug like properties. Relying on the topological polar surface area (TPSA), [55] all compounds exhibit computational TPSA values between 54.02 and 120.50 $Å^2$ and have good intestinal absorption. Besides, absorption (% ABS) was estimated by using the equation % ABS = 109 – (0.345 x TPSA), [56] founding that, the calculated % ABS of all these hits ranged

between 67.42% and 90.36 %. The good ABS % demonstrated that, these hits may have the required cell membrane permeability and bioavailability. It is apparent that, all the derivatives have high gastro-intestinal absorption. Along with, most of them have no permeation to the blood brain barrier, which outweighed that, these systemically targeted molecules will have low to no CNS side effects.

Table 7

Physicochemical properties based on Lipinski´s rule of five and number of rotatable bonds, the topological polar surface area (TPSA), % ABS, GIT absorption and BBB permeability.

Cpd. No.	HBD	HBA	M logP	M.Wt	No. of Rot. bonds	Lipinski´s Violations	TPSA	% ABS	GI Absorption	BBB Permeation
3a	1	5	2.46	398.23	5	0	100.13	74.45	high	No
3b	1	6	2.22	337.32	5	0	100.13	74.45	high	No
3c	1	5	2.34	353.78	5	0	100.13	74.45	high	No
4a	1	5	3.35	301.27	5	0	74.68	83.23	high	Yes
4b	1	6	1.97	328.28	6	0	120.50	67.42	high	No
6a	2	4	2.63	331.75	6	0	75.63	82.90	high	Yes
6b	2	3	3.96	370.61	5	0	66.40	86.09	high	Yes
6c	2	3	3.69	350.20	5	0	66.40	86.09	high	Yes
7a	3	3	2.24	302.35	6	0	117.23	68.55	high	No
7b	3	3	2.47	298.34	6	0	78.43	81.94	high	Yes
7c	3	4	0.51	271.27	6	0	91.32	77.49	high	No
14a	2	4	2.73	371.45	7	0	103.87	73.16	high	No
14b	2	3	2.02	324.40	4	0	101.36	74.03	high	No
14c	1	3	2.97	367.46	6	0	75.80	82.84	high	Yes
14d	2	3	1.97	310.37	4	0	101.36	74.03	high	No
14e	1	4	1.69	354.42	6	0	99.59	74.64	high	No
5-FU	2	3	0.32	130.08	0	0	65.72	86.33	high	No

2.3.2. Molecular Docking studies

The transforming growth factor beta receptor type I (TGFBR1) crystal structure with naphthyridine inhibitor (ligand 460) was obtained and downloaded from protein data bank, PDB file ID: 1VJY with resolution of 2.0Å and 303 amino acids (http://www.pdb.org); it is considered as targets for docking simulations. We performed molecular docking studies in a trial to get better understanding of the binding pattern of the new inhibitors, **4b**, **14e** and the lead compound, **tranilast** with TGFβR1 kinase domain. We performed docking simulations using Molecular Operating Environment software 10.2010 (MOE), Chemical Computing Group Inc., Montreal, Quebec, Canada. After download, refinement of TGFBR1 domain and removal of water chain, then redocking of **ligand 460** into the binding site to perform verification process. After that, the lead compound, tranilast and our new hits, **4b** and **14e** are also docked to the same binding site of TGFβR1.

The docked model of the TGFβR1 inhibitor with **ligand 460** showed docking score of -4.81 Kcal/mol and revealed the following binding modes: hydrogen bonding interaction through its naphthyridine nitrogen atom with His283 (1.89 A^0) and another H bonds between pyrazolidine-H and Asp290 (2.27 A^0), arene-H with Ile 211 amino acid. The obtained results are pictured in Fig. 7a, b.

The docked study of **tranilast** revealed better docking score (-5.72 Kcal/mol) than that with the ligand 460 and displayed hydrogen bond (bond length 2.17 Å) between His283 and carbonyl-O. Also, hydrophobic and arene-H interactions were demonstrated in its docking model between anthranilic ring with Leu340 and Val219. Beside, hydrophobic interaction was observed between dimethoxy phenyl ring and Asp290, (Fig. 8a, b). On the other hand, the docked model of 4-nitrobenzamido derivative, **4b** displayed H bonding with the same amino acid His283 as ligand 460, through the carbonyl-O atom of COOH group, an additional H bond (1.72 Å) with Ser287 through the oxygen atom of $COCH_3$ group. In addition to, arene-H interaction between phenyl of anthranilic acid moiety and Ile211 as long as other hydrophobic interactions with TGFβR1binding site through its phenyl moiety and anthranilic ring with the important amino acids, Ile211, Gly286, Val219, Leu340 and Asp351. Compound **4b** docking score energy was -6.33 kcal/mol. These binding modes explained the enhanced activity of **4b,** (Fig. 9a, b). Concerning compound **14e** which is acrylamide bearing 2-aminothiophen-3-carbonitrile fused with cyclopentane derivative, it revealed docking score energy (-6.92 kcal/mol). Also CN-N bonded to His283 via HBA (2.20 A^0) and arene-H interaction of phenyl core and Lys132 together with hydrophobic interactions with Ile211 Gly286, Val219, and Leu340. The obtained results are pictured in Figs. 10a, b. It worth to mention that, overlay docking alignment of TGFβR1 inhibitors, **4b** and **14e** with the **ligand 460** and **tranilast** showed good fitting of all these compounds in the correct binding site of TGFβR1 as illustrated in Table 8 and Fig. 11.

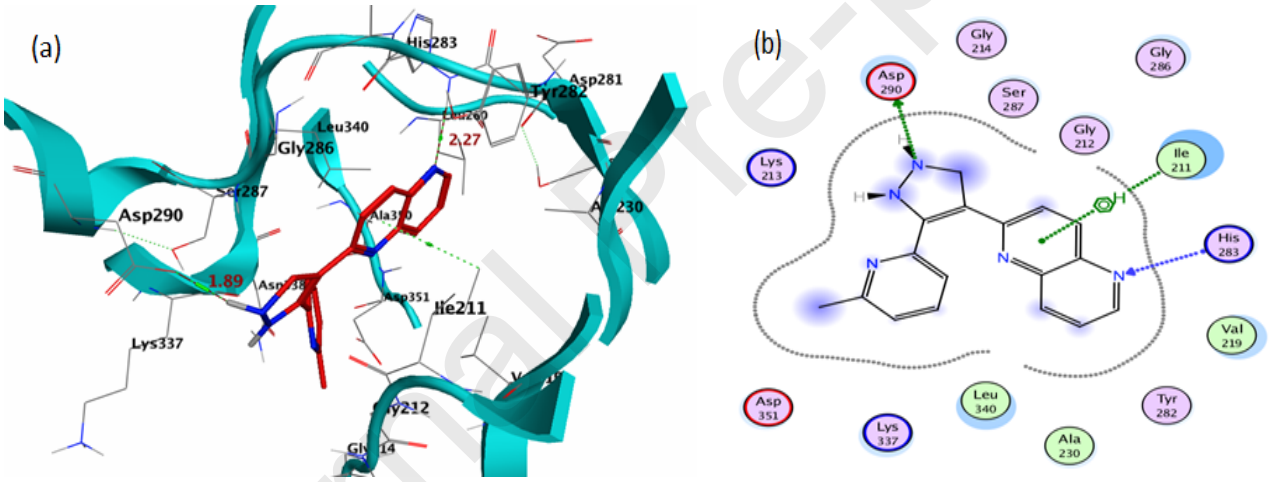

Fig. **7**: (a) 3D and (b) 2D binding interactions of **ligand 460** with TGFβR1 binding site.

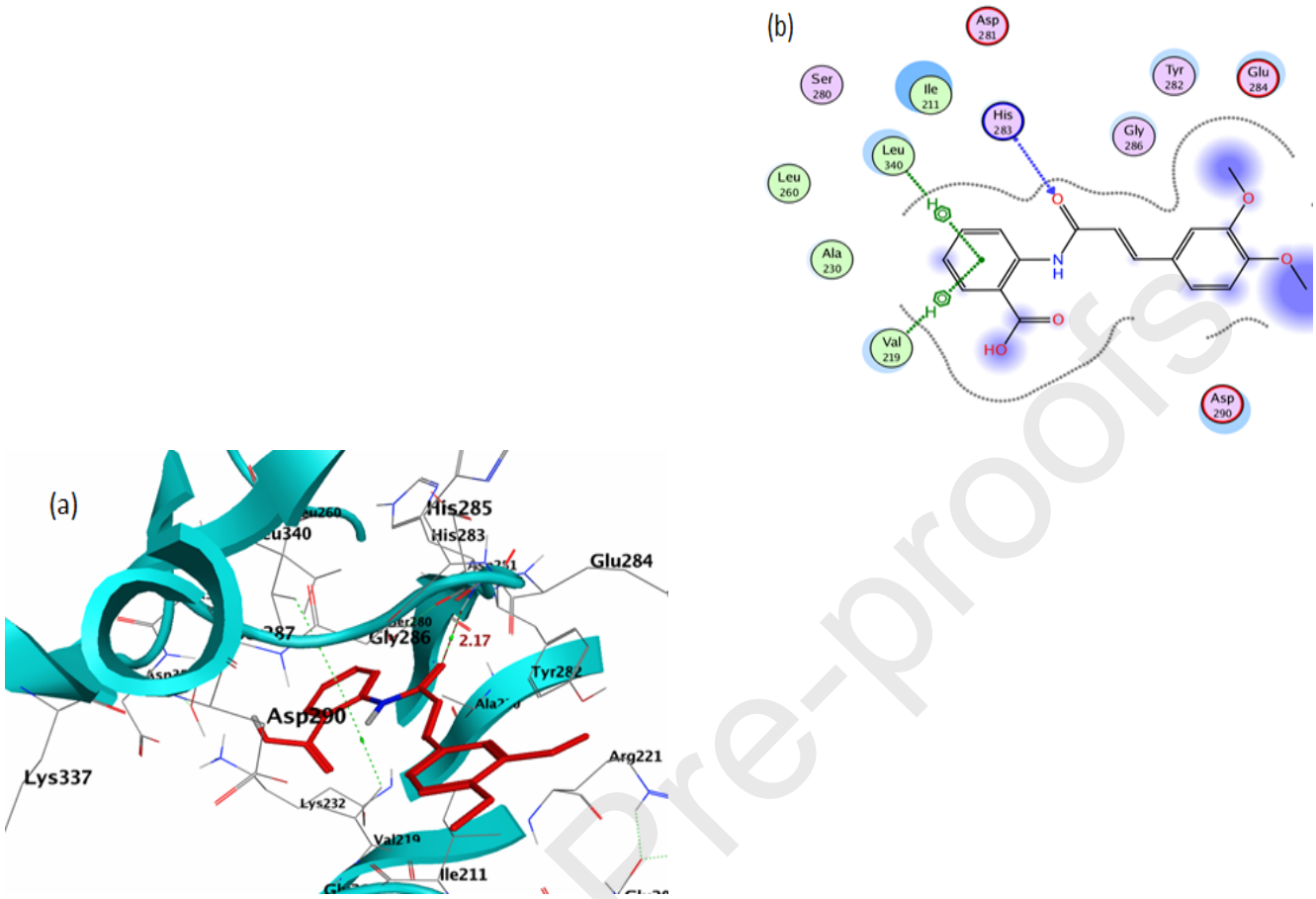

Fig. 8: (a) 3D and (b) 2D binding interactions of **tranilast** with TGFβR1 binding site.

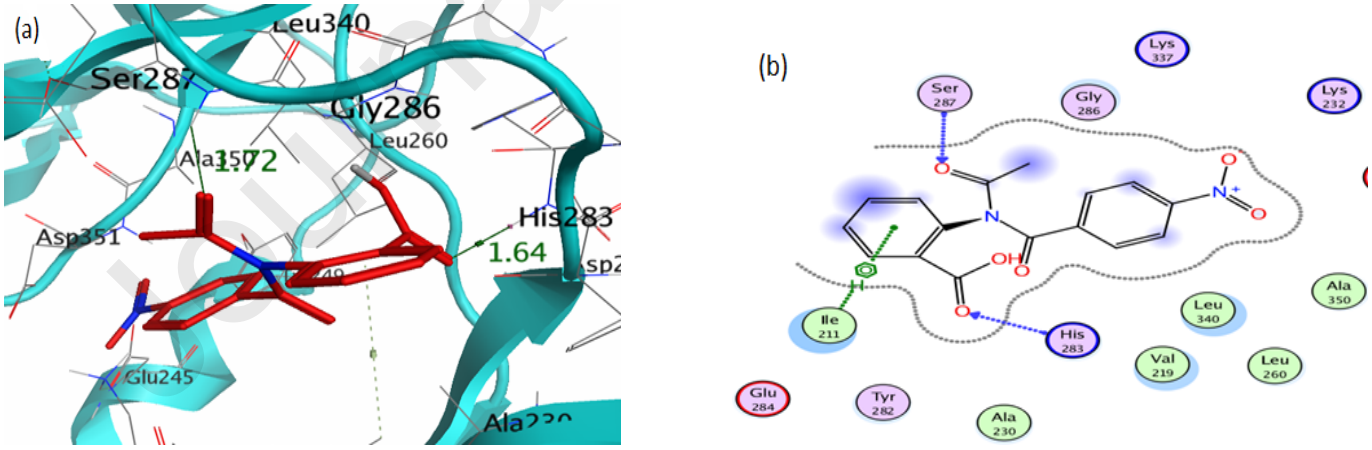

Fig. 9: (a) 3D and (b) 2D binding interactions of compound **4b** with TGFβR1 binding site.

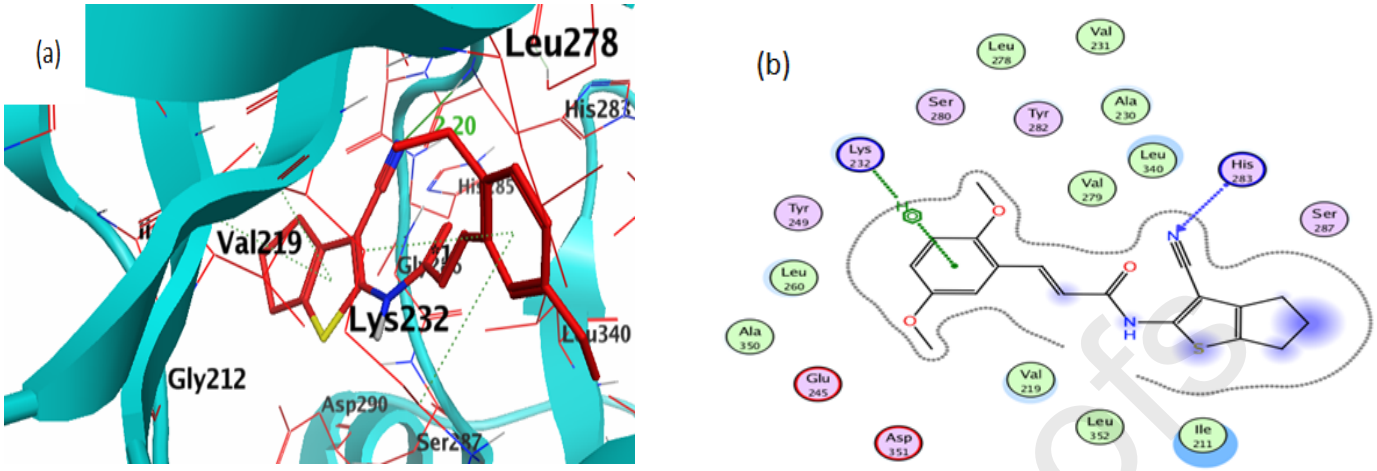

Fig. 10: (a) 3D and (b) 2D binding interactions of compound **14e** with TGFβR1 binding site.

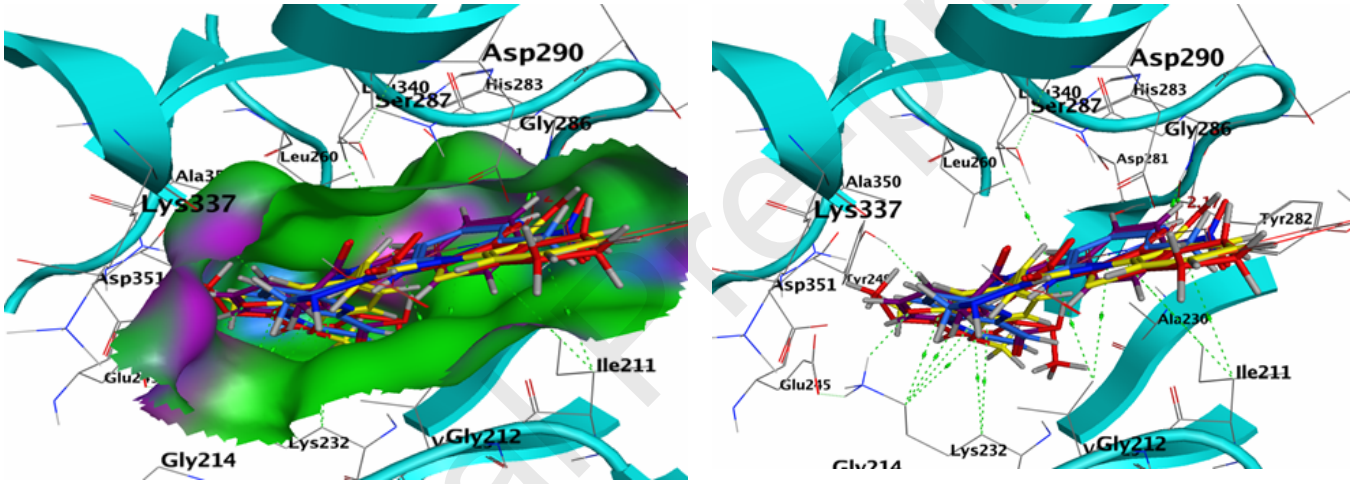

Fig. 11: Overlay docking alignment of Ligand 460 (blue), tranilast (yellow), 4b (purple), and 14e (red) in the active site of TGFβR1 (PDB code: 1VJY).

Table 8
The docking scores (energy) of ligand 460, tranilast, 4b and 14e in the binding pocket of TGFBR1 (PDB: 1VJY)

Cpd. No.	Docking score (Kcal/mol)	No. of H-bonds	Amino acid residues (bond length A^0)	Atoms of cpd.	Type of bonds
Ligand 460	-4.81	2	His283 (2.27);	N1-naphthyridin	H-bond (acceptor)
			Asp290 (1.89);	N-pyrazole	H-bond (donor)
			Ile211	N5-naphthyridin	Arene-H
			Ile211	Naphthyridinyl ring	Hydrophobic
			Leu340	Naphthyridinyl ring	Hydrophobic
			Val219	Naphthyridinyl ring	Hydrophobic
			Asp290	Pyrazole ring	Hydrophobic
Tranilast	-5.72	1	His283 (2.17);	Carbonyl(amide)	H-bond (acceptor)
			Leu340	Anthranilic ring	Arene-H
			VAI219	Anthranilic ring	Arene-H
			Leu340	Anthranilic ring	Hydrophobic
			Val219	Anthranilic ring	Hydrophobic
			Ile211	Anthranilic ring	Hydrophobic

			Aap290	Dimethoxy phenyl	Hydrophobic
4b	-6.33	2	His283 (1.64) Ser287 (1.72); Ile211 Ile211 Val219 Leu340	Carbonyl(acetyl) Carbonyl(acid) Anthranilic ring Anthranilic ring Nitrophenyl Nitrophenyl	H-bond (acceptor) H-bond (acceptor) Arene-H Hydrophobic Hydrophobic Hydrophobic
14e	-6.92	1	His283 (2.20) Lys232 Ile211 Val219 Leu340 Asp290	Nitrile group Dimethoxy phenyl Cyclo pentane Dimethoxy phenyl Thiophene ring Cyclo pentane	H-bond (acceptor) Arene-H Hydrophobic Hydrophobic Hydrophobic Hydrophobic

3. CONCLUSION

In the process of anticancer drug discovery and to find new potential selective anticancer agents, we synthesized a novel series of tranilast analogs. The *in-vitro* anticancer screening of sixteen new synthesized compounds was performed on PC-3, HepG-2 and MCF-7 cell lines using 5-FU as reference drug. Twelve of the investigated compounds showed more potent cytotoxic activity than 5-FU. Particularly, compound **4b** displayed amazing anticancer activity 5-7 times that of reference drug against all the tested cell lines. Six compounds, **4b, 7a, b** and **14c-e,** showed promising cytotoxicity and remarkable selectivity to cancer cells, were further evaluated for their inhibitory activities against TGFβR1. The most active compound, **4b** enhanced apoptosis and arrested G2/M phase of cell cycle. Besides, it induced both caspase-3 level and expression of p53 gene of PC-3 cell. *In silico* study revealed that all target compounds are in agreement with the parameters of Lipiniski's rule. Molecular docking of almost equipotent hits, **4b** and **14e** elicited higher affinities to TGFβR1's binding site with good binding energies compared to ligand 460 and tranilast. Therefore, compounds **4b** and **14e** can be considered as interesting candidates for further development of more potent anticancer agents

4. EXPERIMENTAL PART

4.1. Chemistry

Melting points were measured in open capillary tubes using Griffin apparatus and are uncorrected. Elemental microanalyses were carried out at the Regional Centre for Mycology and Biotechnology, Al-Azhar University. The IR spectra (KBr, cm^{-1}) were recorded using potassium bromide disc technique on a Schimadzu FT/IR 1650 (Perkin Elmer) at Faculty of Pharmacy, Cairo University and Faculty of science, Al-Azhar University.^{1}H NMR (400 MHz) and ^{13}C NMR (100 MHz) spectra (δ, ppm) were performed on Agilent Technologies NMR spectrophotometer at the Armed Forces Laboratories, faculty of pharmacy, Al-Mansoura University and faculty of pharmacy, Ain shams university. DMSO-*d6* was used as a solvent, and the chemical shifts were measured in ppm, relative to TMS as an internal standard. As for the proton magnetic resonance, D_2O was carried out for NH and OH

exchangeable protons. Mass spectra were recorded on a DI-50 unit of EI Shimadzu GC/ MS-QP 2010 plus Spectrometer (Japan) or on single quadrpole EI mass Spectrometer ISQ LT (Thermo scientific) at the Regional Center for Mycology and Biotechnology, Al-Azhar University. All reactions were monitored by TLC using pre-coated Aluminum sheets silica gel Merck 60 F254 and were visualized by UV lamp.

*4.1.1. 2-(N-acetyl-4-substituted benzensulfonyl) benzoic acids (**3a-c**)*

To a solution of N-acetyl anthranilic acid (**2**) (0.01 mol) in ethanol (20 ml), *p*-substituted benzene sulfonyl chlorides (0.01 mol) was added with few dps of TEA. The mixture was heated under reflux from 5-10 h. After completion of the reaction mixture, it was concentrated and allowed to cool then poured into cold water. The precipitate was filtered and crystallized from ethanol to give compounds **3a-c**.

4.1.1.1. 2-(N-acetyl-4-bromobenzensulfonyl) benzoic acid **(3a)**.

Brown powder; Yield (67%); m.p. 172-175^{o}C; IR (KBr, cm^{-1}): 3387 (br, OH), 1709, 1670 (C=O); ^{1}HNMR (400 MHz, DMSO-d_6) δ(ppm): 2.13 (s, 3H, $COCH_3$), 6.63 (t, Ar'-H,1H-3, *J*= 7.6 Hz), 6.83 (d, Ar'-H,1H-5, *J*= 8Hz), 7.29 (t, Ar'-H,1H-4, *J*= 8 Hz), 7.37 (d, Ar-H, 2H-3,5, *J*= 7.6 Hz), 7.52 (d, Ar-H, 2H-2,6 , *J*= 7.6 Hz), 7.73 (d, Ar'-H,1H-2, *J*=7.6 Hz), 11.1 (s, OH, D_2O exchangeable). ^{13}CNMR (DMSO-d_6) δ (ppm): 19.3 (CH_3), 115.6, 121.5, 124.3, 126.3, 129.5, 130.5, 132, 134.2, 138.7(C-SO2) , 142.4 (C-N) , 168 (C=O of amide), 169.4 (C=O of COOH). MS *m/z* (%): 397 (1.96, M^+), 399 (1.95, M^{+2}), 94.9 (100). Anal. Calcd for: $C_{15}H_{12}BrNO_5S$ (397): C, 45.24; H, 3.04; N, 3.52; S, 8.05%, Found: C, 45.64; H, 3.54; N, 3.12; S, 8.39 %.

4.1.1.2. 2-(N-acetyl-4-flouro benzensulfonyl) benzoic acid **(3b)**

Buff powder; Yield (88%); m.p. 193-195^{o}C; IR (KBr, cm^{-1}): 3468 (br, OH), 1716, 1670 (C=O), ^{1}HNMR (400 MHz, DMSO-d_6) δ (ppm): 2.30 (s, 3H, $COCH_3$), 6.94 (t, Ar'-H, 1H-3, *J*= 6 Hz), 7.07 (d, Ar'-H, 1H-5, *J*= 7.2 Hz), 7.15 (t, Ar-H, 2H-3,5, *J*= 6.8 Hz), 7.43 (t, Ar'-H, 1H-4, *J*= 8Hz), 7.65 (t, Ar-H, 2H-2,6, *J*= 6.8 Hz), 7.84 (d, Ar'-H, 1H-2, *J*=8Hz), 11.1 (s, OH, D_2O exchangeable). ^{13}C-NMR (DMSO-d_6) δ (ppm): 19.8 (CH_3), 115.2, 116, 121.5, 124.5, 128.6, 130.5, 134.6, 135.3 (C-SO2), 142.4 (C-N) , 166 (C-F),168 (C=O amide), 169 (C=O of COOH). MS *m/z* (%): 337.04 (3.96, M^+), 94.9(100). Anal. Calcd for $C_{15}H_{12}FNO_5S$ (337.04): C, 53.41; H, 3.59; N, 4.15; S, 9.51%, Found: C, 53.01; H, 3.83; N, 4.57; S, 9.15%.

4.1.1.3. 2-(N-acetyl-4-chlorobenzensulfonyl) benzoic acid **(3c).**

Brown powder; Yield (75%); m.p. 215-218^{o}C; IR (KBr, cm^{-1}): 3421 (br, OH), 1708, 1662 (C=O), ^{1}HNMR (400 MHz, DMSO-d_6) δ (ppm): 2.2 (s, 3H, $COCH_3$), 6.85 (t, Ar'-H, 1H-3, *J*= 7.6 Hz), 7.0 (d, Ar'-H, 1H-5, *J*= 7.6 Hz), 7.16 (t, Ar'-H, 1H-4 , *J*= 8.4 Hz), 7.39 (d, Ar-H, 2H-3,5, *J*= 8.4 Hz), 7.61 (d, Ar-H, 2H-2,6, *J*= 8.4 Hz), 7.81 (d, Ar'-H, 1H-2, *J*= 7.6 Hz), 11.3 (s, OH, D_2O exchangeable). ^{13}C-NMR (DMSO-d_6) δ (ppm): 19.2 (CH_3), 116, 121.5, 124.2, 128.6, 129.2, 130.5, 134.2, 137.5 (C-Cl), 137.8 (C-SO2), 142.4 (C-N), 168 (C=O amide), 169 (C=O of COOH). MS *m/z* (%): 353.01 (3.94, M^+), 355 (1.5, M^{+2}), 65.04 (100). Anal. Calcd for: $C_{15}H_{12}ClNO_5S$ (353.01): C, 50.92; H, 3.42; N, 3.96; S, 9.06%, Found: C, 50.52; H, 3.76; N, 3.64; S, 9.43%.

4.1.2.2-(N-acetyl-4-substituted benzamido)benzoic acids **(4a, b)**

A solution N-acetyl anthranilic acid (**2**) (0.01 mol) and 4-Substituted benzoyl chlorides (0.01 mol) in dry DMF was heated under reflux. The reaction was continued for 6-8 h., and cooled. The precipitate was filtered and crystallized from DMF to afford the target compounds **4a, b**.

4.1.2.1. 2-(N-acetyl-4-fluorobenzamido) benzoic acid **(4a)**

Pale yellow powder; Yield (67%); m.p. 160-162^{o}C; IR (KBr, cm^{-1}): 3367 (br, OH), 1693,1670 and 1654 (C=O); ^{1}HNMR (400 Mz, DMSO-d_6) δ (ppm): 2.11 (s, 3H, CH_3), 7.11 (t, Ar'-H, 1H-3, *J*= 6.8 Hz), 7.3 (t, Ar'-H, 1H-4, *J*= 6.8 Hz), 7.95 (d, 1 Ar'-H,1H-5, *J*= 8 Hz), 8.05 (d, Ar-H, 2H-3,5, *J*= 8 Hz), 8.1 (d, Ar-H, 2H-2,6, *J*= 8 Hz), 8.43 (d, Ar'-H,1H-2, *J*= 8Hz), 11.03 (s, OH, D_2O exchangeable). ^{13}C-NMR(DMSO-d_6) δ (ppm): 20.2 (CH_3), 116, 121.5, 124.2, 129.1, 129.8, 130.5, 134.2, 137.3 (C-N), 166.8 (C-F), 172.1 (CO of amide), 172.3 (C=O of COOH). MS *m/z* (%): 301 (6.96, M^+), 302.19 (5, M^{+2}), 76.04 (100). Anal. Calcd for: $C_{16}H_{12}FNO_4$ (301.01): C, 63.79; H, 4.01; N, 4.65 %, Found: C, 63.45; H, 4.39; N, 4.22 %.

4.1.2.2. 2-(N-acetyl-4-nitrobenzamido) benzoic acid **(4b)**

Pale yellow powder; Yield (54%); m.p. 224-227^{o}C; IR (KBr, cm^{-1}): 3367 (br, OH), 1710,1700 and 1685 (C=O); ^{1}HNMR (400 Mz, DMSO-d_6) δ (ppm): 2.11(s, 3H, CH_3), 7.11 (t, Ar'-H, 1H-3, *J*= 7.2 Hz), 7.54 (t, Ar'-H, 1H-4, *J*= 7.2 Hz), 7.94 (d, Ar'-H,1H-5, *J* = 8Hz), 8.15 (d, Ar-H, 2H-3,5, *J*= 6.8 Hz), 8.3 (d, Ar-H, 2H-2,6, *J*= 6.8 Hz), 8.43 (d, Ar'-H,1H-2, *J*= 8Hz), 11.03 (s, OH, D_2O exchangeable). ^{13}C-NMR (DMSO-d_6) δ (ppm): 20.2 (CH_3), 115.6, 121.2, 124.3, 128.4, 130.5, 134.2, 137.5 (C-N), 140.3, 151.5 (C-NO2), 172.1 (CO of amide), 172.3 (C=O of COOH). MS *m/z* (%): 328.43 (9.35, M^+), 65.01 (100). Anal. Calcd for: $C_{16}H_{12}N_2O_6$ (328.43): C, 58.54; H, 3.68; N, 8.53 %, Found: C, 58.15; H, 3.32; N, 8.82 %.

4.1.3. 2-(2-Chloro-3-(aryl) acrylamido)benzoic acids **(6a-c)**

A mixture of equimolar amounts of 2-chloroacetamido benzoic acid (**5**) and the corresponding aldehydes or acetophenone, namely, 4-methoxy benzaldehyde, 2, 4-dichloro benzaldehyde or 4-chloro acetophenone was reacted in ethanol (20ml)/ TEA under reflux for 8-12 h. The reaction poured into cold water. The precipitate was filtered and washed with water, then crystallized from ethanol to give compounds **6a-c** respectively.

4.1.3.1. 2-(2-Chloro-3-(4-methoxyphenyl) acrylamido) benzoic acid **(6a)**

Brown powder; Yield (65%); m.p. 168-170 ^{o}C; IR (KBr, cm^{-1}): 3251 (br, OH, NH), 1705, 1661 (C=O); ^{1}HNMR (400 MHz, DMSO-d_6) δ (ppm): 3.88 (s, 3H, OCH_3), 6.84 (d , Ar-H, 2H-3,5, *J*= 8 Hz), 7.13 (d, Ar H, 2H-2,6, *J*= 8 Hz), 7.19 (t, Ar'-H, 1H-3, *J*= 12 Hz), 7.53 (s, 1H, Cl-C=CH), 7.69 (t, Ar'-H, 1H-4, *J*=12 Hz), 7.85 (d, Ar'-H, 1H-5, *J*=12 Hz), 7.92 (d, Ar'-H,1H-2, *J*=12 Hz), 8.12 (s, NH, D_2O exchangeable), 9.9 (s, OH, D_2O exchangeable). ^{13}C-NMR (DMSO-d_6) δ (ppm): 56 (OCH_3), 114.2, 115.6, 121.2, 124.3, 126.6 (C-Cl), 127.4, 127.5, 130.5, 134.2, 135.5 (C=C-Cl), 140.7(C-N), 159.9 (C-OCH_3), 163.8 (CO of amide), 169.4

(C=O of COOH). MS *m/z*: 331.37 (23.43, M^+), 333.3 (8.13, M^{+2}), 72.48 (100). Anal. Calcd for: $C_{17}H_{14}ClNO_4$ (331.37): C, 61.55; H, 4.25; N, 4.22 %, Found: C, 61.12; H, 4.63; N, 4.56 %.

4.1.3.2. 2-(2-Chloro-3-(2,4-dichlorophenyl) acrylamido) benzoic acid **(6b)**

Dark brown powder; Yield (42%); m.p. 140-142°C; IR (KBr, cm^{-1}): 3400 (br, OH, NH), 1705, 1695 (C=O); ^{1}HNMR (400 MHz, DMSO-d_6) δ (ppm): 7.24-7.28 (m, Ar-H, 2H-5,6), 7.32-7.39 (m, Ar-H, 1H-3, Ar'-H, 1H-3), 7.64 (t, Ar'-H, 1H-4, *J*= 12 Hz), 7.81 (s, 1H, Cl-C=CH), 7.95 (s, NH, D_2O exchangeable), 8.08 (d, Ar'-H, 1H-5, *J*=12 Hz), 8.66 (d, Ar'-H, 1H-2, *J*=12 Hz), 10.4 (s, OH, D_2O exchangeable). ^{13}C-NMR (DMSO-d_6) δ (ppm): 115.6, 121.2, 124.3, 126.6 (C-Cl), 127, 130.3, 130.5, 131.2, 132.6, 134.2, 134.9, 135.5 (C=C-Cl), 140.7(C-N), 163.8 (CO of amide), 169.4 (C=O of COOH). MS *m/z*: 369.27 (20.41, M^+), 371.86 (6.5, M^{+2}), 373.01 (8.77, M^{+4}), 374.95 (5.28, M^{+6}), 85.91 (100). Anal. Calcd for: $C_{16}H_{10}Cl_3NO_3$ (369.27): C, 51.85; H, 2.72; N, 3.78 %, Found: C, 51.45; H, 2.35; N, 3.43 %.

3.1.3.3. 2-(2-Chloro-3-(4-chlorophenyl) but-2-enamido) benzoic acid **(6c)**

Dark brown powder; Yield (68%); m.p.230-233°C; IR (KBr, cm^{-1}): 3349, 3271 (br, OH, NH), 1705, 1687 (C=O); ^{1}HNMR (400 MHz, DMSO-*d6*) δ (ppm): 2.56 (s, 3H, CH_3), 7.37 (d, Ar-H, 2H-2,6, *J*=12 Hz), 7.52 (t, Ar'-H, 1H-3, *J*= 8 Hz), 7.66 (d, Ar-H, 2H-3,5, *J*= 12 Hz), 7.77 (t, Ar'-H, 1H-4, *J*= 8 Hz), 7.99 (d, Ar'-H, 1H-5, *J*= 12 Hz), 8.12 (s, NH, D_2O exchangeable), 8.42 (d, Ar'-H, 1H-2, *J*= 12 Hz),11.01 (s, OH, D_2O exchangeable). ^{13}C-NMR (DMSO-d_6) δ (ppm): 11.7 (CH_3), 115.6, 119.2 (C-Cl), 121.2, 124.3, 127.8, 128.8, 130.5, 133.5, 134.2, 140.7(C-N), 144.9 (C-CH3), 163.8 (CO of amide), 169.4 (C=O of COOH). MS *m/z*: 349.14 (8.53, M^+), 351.35 (2.27, M^{+2}), 86.03 (100). Anal. Calcd for $C_{17}H_{13}Cl_2NO_3$ (349.14): C, 58.31; H, 3.74; N, 4.00 %, Found: C, 58.65; H, 3.42; N, 4.32 %.

4.1.4.2-(2-(Aryl/ heteroarylamino) acetamido) benzoic acids **(7a-c)**

Equimolar amounts of 2-chloroacetamido benzoic acid (**5**) and different substituted amines, (2-amino thiophenol, 2,4-dimethyl aniline and 4-amino pyridine) were refluxed in ethanol in presence of few drops of TEA for 8-12 h. The reaction mixture was cooled poured into cold water. The precipitate was filtered, and crystalized from ethanol to afford the compounds **7a-c**.

4.1.4.1. 2-(2-(2-Mercaptophenylamino) acetamido) benzoic acid **(7a)**

Yellowish green powder; Yield (67%); m.p. 145-147°C; IR (KBr, cm^{-1}): 3448 (br, OH), 3352, 3309 (NH), 1710, 1662 (C=O); ^{1}HNMR (400 Mz, DMSO-d_6) δ (ppm):3.41(s, 1H, SH), 4.18-4.22 (m, 2H, CH_2), 5.25 (s, NH, D_2O exchangeable), 6.38-6.42 (m, Ar-H, 2H-4,6), 6.47-6.53 (m, Ar-H, 2H-3,5), 7.06 (s, NH, D_2O exchangeable), 6.92-6.97 (m, Ar'-H, 2H-3,5), 7.14 (t, Ar'-H, 1H-4, *J*= 7.6 Hz), 7.29 (d, Ar'-H,1H-2, *J*= 7.2Hz),10.52 (s, OH, D_2O exchangeable). ^{13}C-NMR (DMSO-d_6) δ (ppm): 54.8 (CH_2), 113.4, 115.6, 116.3, 117.5, 121.5, 124, 126.4, 130.2, 130.5, 134.2, 143.3 (C-N), 144.5, 168.5 (CO amide), 169.4 (C=O of COOH). MS *m/z* (%): 302 (44, M^+), 64.09 (100). Anal. Calcd for: $C_{15}H_{14}N_2O_3S$ (302.07): C, 59.59; H, 4.67; N, 9.27; S, 10.61 %, Found: C, 59.25; H, 4.33; N, 9.65; S, 10.28 %.

4.1.4.2. 2-(2-(2, 4-Dimethylphenylamino) acetamido)benzoic acid **(7b)**

Brown powder; Yield (53%); m.p. 223-225°C; IR (KBr, cm^{-1}): 3447 (br, OH), 3381 (NH), 1685, 1605(C=O); ^{1}HNMR (400 Mz, DMSO-d_6) δ (ppm): 2.2 (s, 3H, CH_3), 2.3 (s, 3H, CH_3), 4.49-4.51 (m, 2H, CH_2, NH, D_2O exchangeable), 7.1 (d , Ar-H, 1H-6, *J*= 4 Hz), 7.22 (s, Ar-H, 1H-3), 7.24 (d, Ar-H, 1H-5, *J*= 4 Hz), 7.52 (t, Ar'-H, 1H-3, *J*= 20 Hz), 7.78 (t, Ar'-H, 1H-4, *J*= 20 Hz), 8.09 (d, Ar'-H, 1H-5, *J*= 8 Hz), 8.21 (s, NH, D_2O exchangeable), 8.33 (d, Ar'-H, 1H-2, *J*= 20 Hz), 11.36 (s, OH, D_2O exchangeable). ^{13}C-NMR (DMSO-d_6) δ (ppm): 15.8, 24.6 ($2CH_3$), 55.5(CH_2) 113.3, 115.6, 116, 121.5, 124, 126.9, 130.5, 131.7, 134.2, 143.3 (C-N), 143.5, 168.5 (CO amide), 169.4 (C=O of COOH).MS *m/z* (%): 298.21 (19.84, M^+), 76.23(100). Anal. Calcd for $C_{17}H_{18}N_2O_3$ (298.21): C, 68.44, H, 6.08; N, 9.39%, Found: C, 68.17, H, 6.43; N, 9.62 %.

4.1.4.3. 2-(2-(Pyridin-4-ylamino) acetamido) benzoic acid **(7c)**

Buff powder; Yield (42%); m.p. 276-279°C; IR (KBr, cm^{-1}): 3350 (br, OH), 3200 (NH), 1670, 1651(C=O); ^{1}HNMR (400 Mz, DMSO-d_6) δ (ppm): 4.31-4.34 (m, 2H, CH_2, NH D_2O exchangeable), 6.83 (d, Ar-H, 2H-2,6 of pyridine, *J*= 7.2 Hz), 6.94 (t, Ar'-H, 1H-3, *J*= 8 Hz), 7.24 (t, Ar'-H, 1H-4, *J*= 8 Hz), 7.95 (d, Ar'-H, 1H-5, *J*= 8 Hz) , 8.12 (d, Ar-H, 2H-3,5 of pyridine, *J*= 7.6 Hz), 8.18 (s, NH, D_2O exchangeable), 8.32 (d, Ar'-H, 1H-2, *J*= 7.6 Hz), 15.5 (s, OH, D_2O exchangeable). ^{13}C-NMR (DMSO-d_6) δ (ppm): 55 (CH_2), 109.1, 115.6, 121.5, 124, 130.5, 134.2, 143.3 (C-N), 150.5, 155, 168.5 (CO amide), 169.4 (C=O of COOH). MS *m/z* (%): 271.1(7.42, M^+), 65.04 (100). Anal. Calcd for $C_{14}H_{13}N_3O_3$ (271.1): C, 61.99; H, 4.83; N, 15.49 %, Found: C, 61.55; H, 4.47; N, 15.17 %.

4.1.5. Acrylamides **(14a-e)**

Equimolar amounts of substituted amino thiophenes (**10a-c**) and substituted cinnamoyl chlorides (**13a,b**) namely: 4-hydroxycinnamoyl or 2,5-dimethoxycinnamoyl chloride were refluxed in acetone in presence of anhydrous K_2CO_3 for 5-8 h. The reaction medium was cooled and poured into acidified water. The precipitate was filtered, dried and crystalized from ethanol.

4.1.5.1. Ethyl-2-((E)-3-(4-hydroxyphenyl)acrylamido)-4,5,6,7tetrahydrobenzo[b]thiophene-3-carboxylate **(14a)**

Buff powder; Yield (79%); m.p. 116-118 °C; IR (KBr, cm^{-1}): 3404, 3298 (OH, NH), 1745, 1646 (C=O); ^{1}HNMR (400 MHz, DMSO-d_6) δ (ppm): 1.24 (t, 3H, CH_3, *J*= 8 Hz), 1.62-1.68 & 2.50-2.56 (m, 8H, CH_2 of Cyclohexane), 4.14 (q, 2H, OCH_2, *J*= 8 Hz), 5.2 (s, OH, D_2O exchangeable). 6.84 (d , Ar-H, 2H-3,5, *J*= 8 Hz), 7.22 (d, olefinic, 1H-y, *J*= 16 Hz), 7.73 (d, Ar-H, 2H-2,6, *J*= 8 Hz), 7.96 (d, olefinic,1H-x, *J*= 16 Hz), 8.12 (s, NH, D_2O exchangeable). ^{13}C-NMR (DMSO-d_6) δ (ppm): 15 (CH_3), (20, 23.5, 25 cyclohexane), 61(OCH_2), 97.6, 115.8, 119.1, 126.5, 127.4, 127.8, 144, 157.5 (C-OH) , 155, 160.4 (C=O of COOR),166.7 (CO of amide), 176(C-S). MS *m/z*: 371.12 (21.53%, M^+). Anal. Calcd for: $C_{20}H_{21}NO_4S$ (371.12): C, 64.67; H, 5.70; N, 3.77; S, 8.63 %, Found: C, 64.22; H, 5.35; N, 4.01; S, 8.43 %

4.1.5.2. (E)-N-(3-cyano-4,5,6,7-tetrahydrobenzo[b]thiophen-2-yl)-3-(4-hydroxyphenyl)acrylamide **(14b)**

Buff powder; Yield (82%); m.p. 268-270 °C; IR (KBr, cm-^{1}): 3322, 3257 (OH, NH), 2204(C≡N), 1633 (C=O); ^{1}HNMR (400 MHz, DMSO-d_6) δ (ppm): 1.64-1.69 & 2.40-2.48 (m, 8H, CH_2 of Cyclohexane), 4.99 (s, OH, D_2O exchangeable). 6.88(d , Ar-H, 2H-3,5, *J*= 8 Hz), 7.25 (d, olefinic, 1H-y, *J*= 16 Hz), 7.67 (d, Ar-H, 2H-2,6, *J*= 8 Hz), 7.91 (d, olefinic,1H-x, *J*= 16 Hz), 8.1 (s, NH, D_2O exchangeable). ^{13}C-NMR (DMSO-d_6) δ (ppm): (19.4, 23, 23.5, 24.5 cyclohexane), 67.5(C-CN), 115.5 (C≡N), 115.8, 119.1, 126.5, 127, 127.8, 135, 144, 146.5(S-C-N), 157.5 (C-OH), 166.5 (CO of amide). MS *m/z*: 324.09 (M^+). Anal. Calcd for: $C_{18}H_{16}N_2O_2S$ (324.09): C, 66.64; H, 4.97; N, 8.64; S, 9.88 %, Found: C, 66.23; H, 4.55; N, 8.87; S, 9.58 %

4.1.5.3. (E)-N-(3-cyano-4,5,6,7-tetrahydrobenzo[b]thiophen-2-yl)-3-(2,5-dimethoxyphenyl)acrylamide **(14c)**

Brown powder; Yield (85%); m.p. 99-102 ^{o}C; IR (KBr, cm^{-1}): 3220 (NH), 2203(C≡N), 1645 (C=O); ^{1}HNMR (400 MHz, DMSO-d_6) δ (ppm): 1.64-1.69 & 2.44-2.51 (m, 8H, CH_2 of Cyclohexane), 3.88 (s, 6H, 2OCH_3), 6.76 (d , Ar-H, 1H-4, *J*= 7.6 Hz), 7.21 (d, Ar-H, 1H-3, *J*= 8 Hz), 7.33 (d, olefinic, 1H-y, *J*= 16 Hz), 7.43 (s, Ar-H, 1H-6), 8.01 (s, NH, D_2O exchangeable), 8.03 (d, olefinic,1H-x, *J*= 16 Hz). ^{13}C-NMR (DMSO-d_6) δ (ppm): (19.4, 23, 23.5, 24.5 cyclohexane), 55.9(, 56.5 (2OCH_3), 68(C-CN),111.2, 114, 115.5 (C≡N), 115.8, 117, 129, 135.5, 144, 146.5(S-C-N), 150, 153, 166.7 (CO amide). MS *m/z*: 368.45 (M^+). Anal. Calcd for: $C_{20}H_{20}N_2O_3S$ (368.45): C, 65.20; H, 5.47; N, 7.60; S, 8.70 %, Found: C, 65.67; H, 5.12; N, 7.93; S, 8.32 %

4.1.5.4. (E)-N-(3-cyano-5,6-dihydro-4H-cyclopenta[b] thiophen-2-yl)-3-(4-hydroxyphenyl)acrylamide **(14d)**

Black powder; Yield (64%); m.p. 132-134 ^{o}C; IR (KBr, cm^{-1}): 3334, 3219 (OH, NH), 2193 (C≡N), 1650 (C=O); ^{1}HNMR (400 MHz, DMSO-d_6) δ (ppm): 1.92-1.96 & 2.43-2.50 (m, 6H, CH_2 of Cyclopentane), 5.22 (s, OH, D_2O exchangeable), 6.67 (d , Ar-H, 2H-3,5, *J*= 8 Hz), 6.98 (d, olefinic, 1H-y, *J*= 16 Hz), 7.49 (d, Ar-H, 2H-2,6, *J*= 8 Hz), 7.88 (d, olefinic,1H-x, *J*= 16 Hz), 8.1 (s, NH, D_2O exchangeable). ^{13}C-NMR (DMSO-d_6) δ (ppm): (21.2, 25.5, 31.9 cyclopentane), 67.5(C-CN), 115.3 (C≡N), 115.8, 118.9, 127, 127.8, 129, 135.4, 144, 146.5(S-C-N), 157.7 (C-OH), 166.7 (CO of amide). MS *m/z*: 310.37 (M^+). Anal. Calcd for: $C_{17}H_{14}N_2O_2S$ (310.37): C, 65.79; H, 4.55; N, 9.03; S, 10.33 %, Found: C, 65.79; H, 4.55; N, 9.03; S, 10.33 %

4.1.5.5. (E)-N-(3-cyano-5,6-dihydro-4H-cyclopenta[b]thiophen-2-yl)-3-(2,5-dimethoxyphenyl)acrylamide **(14e)**

Pale brown powder; Yield (55%); m.p. 264-266^{o}C; IR (KBr, cm^{-1}): 3170 (NH), 2201(C≡N), 1647 (C=O); ^{1}HNMR (400 MHz, DMSO-d_6) δ (ppm): 1.88-1.96 & 2.38-2.46 (m, 6H, CH_2 of Cyclopentane), 3.84 (s, 6H, 2OCH_3), 6.64 (d , Ar-H, 1H-4, *J*= 7.6 Hz), 7.38 (d, Ar-H, 1H-3, *J*= 8 Hz), 7.47 (d, olefinic, 1H-y, *J*= 16 Hz), 7.51 (s, Ar-H, 1H-6), 8.87 (d, olefinic,1H-x, *J*= 16 Hz), 7.99 (s, NH, D_2O exchangeable). ^{13}C-NMR (DMSO-d_6) δ (ppm): (21.2, 25.5, 31.9 cyclopentane), 55.9, 56.3 (2OCH_3), 67.5(C-CN), 111.6, 114.5, 115.2, 115.3 (C≡N), 116, 118.9, 129, 135.4, 144, 146.8 (S-C-N), 150, 152.8 (2C-OCH_3), 166.7 (CO of amide). MS *m/z*: 354.42 (M^+). Anal. Calcd for: $C_{19}H_{18}N_2O_3S$ (354.42): C, 64.39; H, 5.12; N, 7.90; S, 9.05 %, Found: C, 64.62; H, 5.45; N, 7.46; S, 9.55 %**.**

4.2. Biological activities.

4.2.1. In vitro anti-proliferative activities

Cancer cells from different cancer cell lines; Human prostate carcinoma cell lines (PC-3), hepatocellular carcinoma cell lines (HepG-2) and human breast adenocarcinoma cell line (MCF-7) were obtained from VACSERA- Cell Culture Unit, Cairo, Egypt. Also, the cytotoxic evaluation of all compounds against normal cells WI-38 was carried out to explore the toxicity and selectivity of the tested compounds. For comparison, 5-FU was used as a standard reference drug. Anti-proliferative activities of the synthesized compounds were carried out based on MTT assay. [48] Briefly, human cancer cell lines were dropped in 96-well plates at a density of $3^{-8}\times10^3$ cells/well. Next, the wells were incubated for 12 h in a 5% CO_2 incubator at 37 °C. Then, for each well, the growth medium was exchanged with 0.1 mL of fresh medium containing graded concentrations of the test compounds to be or equal DMSO and incubated for two days. Then 10 µl MTT solutions (5µg/ml) was added to each well, and the cells were incubated for additional 4 h. The crystals of MTT-formazan were dissolved in 100 µl of DMSO; the absorbance of each well was measured

at 490 nm using an automatic ELISA reader system (TECAN, CHE). The IC_{50} values were calculated using the nonlinear regression fitting models (Graph Pad, Prism Version 5). The means of at least three separate experiments gave the reported results. Statistical differences were analyzed according to one-way ANOVA test wherein the differences were considered to be significant at $p < 0.05$.

4.2.2. Determination of TGFBR1 activity

The effects of the synthesized compounds on the activity of TGFβR1 were measured using Human TGF-beta1 ELISA (Enzyme-Linked immunosorbent Assay) kit (Catalog #: ELH-TGFb1). The kit was activated by adding 0.1 ml 1 N HCI into 0.5 mL cell culture supernatant. Incubated for 10 minutes at r.t., neutralized by adding 0.1 ml 1.2 N NaOH/0.5 M HEPES (PH=7.0~7.6), then diluted with 1X Assay Diluent (Item E2) and assayed immediately according to the manufacturer's instructions. Shortly, the assay was performed using 100 mL of the cells supernatant in each well, which were incubated for 2.5 h. at r.t, followed by adding 100 µl biotin antibody (incubated for 1 hr at r.t), 100 µl prepared Streptavidin solution (Incubate 45 minutes at r. t.) and 100 µl TMB One-Step Substrate Reagent to each well (Incubate 30 minutes at r. t.). Finally, 50 µl Stop Solution was added to each well, the optical density of each well was determined within 5 min using a microplate reader set at 450 nm.

4.2.3. Cell cycle analysis

PC-3 cells were seeded in a 6-well plate at concentration of 1 X 10^5 cells per well, then incubated for 24 h. The cells were treated with (0.1% DMSO) vehicle or 0.36 µg/ml of compound **4b** for 24 h. After that, the cells were harvested and fixed for 12 h using ice-cold 70% ethanol at 4 ^oC. Removal of ethanol and washing cells with cold PBS was done. Then, the cells were incubated in 0.5 ml of PBS containing 1 mg/mL RNase at 37^oC for 30 min. The cells were stained for 30 min with propidium iodide in the dark. Afterwards, the flow cytometer was used to detect DNA contents. [49]

4.2.4. Apoptosis detection studies

4.2.4.1. Annexin-V assay

PC-3 cells were seeded in a 6-well plate (1X10^5cells/well), incubated for 24 h, and then treated with vehicle (0.1% DMSO) or 0.36 µg/ml of compound **4b** for 24 h. Subsequently, the cells were harvested, washed using PBS and stained for 15 min at room temperature in the dark using annexin V-FITC and PI in binding buffer (10 mM HEPES, 140 mM NaCl and 2.5 mM $CaCl_2$ at pH 7.4), then analyzed by the flow cytometer. [50]

4.2.4.2. Determination of the active caspase-3

To determine the effect of test compounds on apoptosis, the active caspase-3 level was measured by using Quantikine-Human active Caspase-3 Immunoassay (R&D Systems, Inc. Minneapolis, USA) according to the manufacturer protocol. Briefly, after washing the PC-3 cells with PBS, the cells were collected and lysed by adding it to the extraction buffer containing protease inhibitors (1 mL per 1 x 10^7 cells.) then, the lysate was diluted immediately prior to the assay. At the end of the assay, the optical density of each well was determined within 30 min using a microplate reader set at 450 nm.

4.2.4.3. Determination of the gene expression of some apoptosis key marker (p53)

The effect of compound **4b** on the gene expression of apoptosis marker (p53) was measured using p53 *in vitro* Simple Step ELISA® kit (Catalog #: ab171571). All materials and prepared reagents were kept at room temperature prior to use. Briefly, the assay was performed using 50 µl samples and standards to appropriate wells, followed by adding 50 µL of the Antibody Cocktail. The plate was sealed, covered and incubated for 1 h at room temperature on a plate shaker set to 400 rpm. After washing the PC-3 cells with 3 x 350 µL 1X Wash Buffer PT, 100 µl TMB, One-Step Substrate Reagent was added to each well (Incubate 10 minutes at r. t. in the dark). Finally, 100 µl Stop Solution was added to each well and the optical density of each well was determined within 5 min using a microplate reader set at 450 nm.

4.3. Molecular Modeling:

4.3.1. In silico physicochemical and ADME properties prediction

The molecular structures were converted into SMILES database using Chemdraw 12.0. Then, these SMILES were inserted as input in SwissADME website to calculate the physicochemical descriptors, lipophilicity, pharmacokinetics properties, ADME parameters, and medicinal chemistry friendliness.

4.3.2. Docking Studies

Crystallographic structures of TGFBR1 was retrieved from Protein Data Bank [PDB ID: 1VJY, with resolution of 2.0Å and 303 amino acids (http://www.pdb.org), and considered as targets for docking simulations. The docking analysis was performed using MOE software to evaluate the free energies and binding mode of the designed molecules against TGFBR1. At first, the crystal structures of TGFBR1was prepared by removing water molecules and retaining only one chain and its co-crystallized ligand, naphthyridine. Then, the protein structure was protonated and the hydrogen atoms were hided. Next, the energy was minimized and the binding pocket of the protein was defined. The 2D structures of the synthesized compounds and the co-crystallized ligand, naphthyridine were sketched using ChemBioDraw Ultra 12.0 and saved as MDL-SD format. After that, the saved files were opened using MOE, 3D structures were protonated and energy minimization was applied. Before docking the synthesized compounds, validation of the docking protocol was carried out by running the simulation using the co-crystallized ligand and low RMSD between docked and crystal conformations. The molecular docking of the synthesized compounds and the co-crystallized ligand was performed using a default protocol. In each case, four docked structures were generated using genetic algorithm searches.

5. REFERENCES:

[1] Kubiczkov L., Sedlarikov L., Hajek R. and Sevcikov., " TGF-β – an excellent servant but a bad master ", *Journal of Translational Medicine*, 10:183, **2012**.
[2] Mahdy H. A., Ibrahim M. K., Metwaly A. M., Belal A., Mehany A. B. M., El-Gamal K. M. A., El-Sharkawy A., Elhendawy M., Radwan M. M., El sohly M. A. , Eissa I. H. "Design, synthesis, molecular modeling, *invivo* studies and anticancer evaluation of quinazolin-4(3H)-one derivatives as potential VEGFR-2 inhibitors and apoptosis inducers ", *Bioorganic Chemistry*, 94, 103422, **2020**.
[3] WHO, Cancer, fact sheet, 2018, 2018.< http://www.who.int/news-room/factsheets/detail/cancer > (Accessed September **2018**.
[4] Nacif M. and Shaker O., " Targeting Transforming Growth Factor-β (TGF-β) in Cancer and Non-Neoplastic Diseases ", *Journal of Cancer Therapy,* (5), 735-747, **2014**.
[5] Derynck R. and Zhang Y. E., "Smad-dependent and Smad-independent pathways in TGFb family signalling", *Nature puplishing group, |www.nature.com/nature,* (425), **2003**.
[6] Baugé C., Cauvard O., Leclercq S., Galéra P., Boumédiene K., " Modulation of transforming growth factor beta signalling pathway genes by transforming growth factor beta in human osteoarthritic chondrocytes: involvement of Sp1 in both early and late response cells to transforming growth factor beta ", *Arthritis Research & Therapy,* 13:R23, , **2011**.
[7] Akhurst R. J. and Hata A., "Targeting the TGFβ signaling pathway in disease", *Nature Reviews Drug Discovery,* (11), 790-811, **2012**.
[8] Geldenhuys W. J. and Nakamura H., "3D-QSAR and docking studies on transforming growth factor (TGF)-b receptor 1 antagonists ", *Bioorganic & Medicinal Chemistry Letters*, 20, 1918–1923, **2010**.

[9] Neuzillet C., Gramont A. d., Raballand A. T., Mestier L. d., Cros J., Faivre S. and Raymond E. "Perspectives of TGF-β inhibition in pancreatic and hepatocellular carcinomas", Oncotarget, 5(1), 78-94, **2013**.
[10] Yingling J. M., McMillen W. T., Yan L., Huang H., Sawyer J. S., Graff J., Clawson D. K., Britt K. S., Anderson B. D., Beight D. W., Desaiah D., Lahn M.l M., Benhadji K. A., Lallena M. J., Holmgaard R. B., Xu X., Zhang F., Manro J. R., Iversen P. W., Iyer C. V., Brekken R. A., Kalos M. D. and Driscoll K. E., "Preclinical assessment of galunisertib (LY2157299 monohydrate), a first-in-class transforming growth factor-β receptor type I inhibitor . " *oncotarget* , 9(6), 6659-6677, **2018**.
[11] Byfield S. D., Major C., Laping N. J., and Roberts A. B. "SB-505124 Is a Selective Inhibitor of Transforming Growth Factor- Type I Receptors ALK4, ALK5, and ALK7", *Mol Pharmacol*, 65, 774-752, **2004**.
[12] Capper E. A., Roshak A. K., Bolognese B. J., Podolin P. L., Smith T., Dewitt D. L., Anderson K. M., and Marshall L. A. "Modulation of human monocyte activities by tranilast, SB 252218, a compound demonstrating efficacy in restenosis", *J. Pharmacol. Exp. Ther*., 295, 1061-1069, **2000**.
[13] Gellibert F., Woolven J., Fouchet M. H., Mathews N., Goodland H., Lovegrove V., Laroze A., Nguyen V., Sautet S., Wang R., Janson C., Smith W., Krysa G., Boullay X V., Gouville A. C., Huet S. and Hartley D., "Identification of 1, 5-Naphthyridine Derivatives as a Novel Series of Potent and Selective TGF-â Type I Receptor Inhibitors", *J. Med. Chem*, 47, 4494-4506, **2004**.
[14] Herbertz S., Sawyer J. S., Stauber A. J., Gueorguieva I., Driscoll K. E., Estrem S. T., Cleverly A. L., Desaiah D., Guba S. C., Benhadji K. A., Slapak C. A.and Lahn M. M., "Clinical development of galunisertib (LY2157299 monohydrate), a small molecule inhibitor of transforming growth factor-beta signaling pathway", *Drug Design, Development and Therapy*, 9, 4479–4499, **2015**.
[15] Raffa D., Maggio B., Plescia F., Cascioferro S., Plescia S., Raimondi M. V., Daidone G., Tolomeo M., Grimaud S., Cristina A. D., Pipitone R. M., Bai R.and Hamel E., "Synthesis, antiproliferative activity, and mechanism of action of a series of 2-{[(2E)-3-phenylprop-2-enoyl]amino}benzamides " *European Journal of Medicinal Chemistry*, 46, 2786-2796, **2011**.
[16] Rogosnitzky M., Danks R. And Kardash E., "Therapeutic Potential of Tranilast, an Anti-allergy Drug, in Proliferative Disorders", *Anticancer Research*, 32, 2471-2478, **2012**.
[17] Isaji M., Miyata H., Ajisawa Y., Takehana Y. and Yoshimura N., "Tranilast inhibits the proliferation, chemotaxis and tube formation of human microvascular endothelial cells in vitro and angiogenesis in vivo", *British Journal of Pharmacology*, 1061 - 1066., 122, 1061-1066, **1997**.
[18] Yashiro M., Murahashi K., Matsuoka T., Nakazawa K., Tanaka H., Osaka H., Koyama T., Ohira M., Chung K. H.," Tranilast (N-3,4-dimethoxycinamoyl anthranilic acid): A novel inhibitor of invasion-stimulating interaction between gastric cancer cells and orthotopic fibroblasts". *Anticancer Res*., 23, 3899 - 3904, **2003**.
[19] SubramaniamV., Chakrabarti R., Prud'homme G. J. and Jothy S., "Tranilast inhibits cell proliferation and migration and promotes apoptosis in murine breast cancer ". *Anti-Cancer Drugs,* 21 (4), 351-361, **2010**.
[20] Pistritto G., Trisciuoglio D., Ceci C., Garufi A., and Orazi G. D., "Apoptosis as anticancer mechanism: function and dysfunction of its modulators and targeted therapeutic strategies", *AGING*, 8 (4), 603-619, **2016**.
[21] Brahmachari G., Laskar S. and Sarkar S., "A green approach to chemoselective N-acetylation of amines using catalytic amount of zinc acetate in acetic acid under microwave irradiation", *Indi. J. of Chemistry*, 49B, 1274-1281, **2010**.
[22] Erikson J., "N-acetylanthranilic acid: a highly triboluminercent material", *J. Chem. Educ*., 49 (10), 688, **1972**.
[23] Kiruthiga B., Ilango K., Valentina P., Umarani N. and Patel R., "synthesis of some new 2-substituted quinazolin-4-one derivatives and their biological activties", *Int. J. Pharm. Tech. Res*., 1(4), 1503-1506, **2009.**
[24] Ismail M. M. F., Amin K. M., Noaman E., Soliman D. H., Ammar Y. A., "New quinoxaline 1, 4-di-N-oxides: Anticancer and hypoxia-selective therapeutic agents", *European Journal of Medicinal Chemistry*, 45, 2733-2738, **2010.**
[25] Pasha M. A., Khan R. R. and Shrivatsa N., "N-Sulfonylation of amines, imides, amides and anilides using p-TsCl in presence of atomized sodium in EtOH-THF under sonic condition", *http://dx.doi.org/10.1016/j.ultsonch*., **2015**.
[26] AL-Zubiady S. and Ibrahim W. A.., "Synthesis and characterization of new quinazoline–4(3H)-one Schiff bases", *J. Chem. Pharm. Res*., 5 (7), 42-45, **2013**.
[27] Thirugnanasambanthan A. and Sankarnarayanan S., "Synthesis of 2, 3-disubstituted quinazolone derivatives for analgesic and antimicrobial activities", *J. Chem. Pharm. Res*., 4 (2), 1147-1150, **2012**.
[28] Ismail M. M. F., Ammar Y. A., El-Zahaby H. S. A., Eisa S. I., and Barakat S. E., "Synthesis of Novel 1-Pyrazolylpyridin-2-ones as Potential Anti-Inflammatory and Analgesic Agents", *Arch. Pharm. Chem. Life Sci*., 340, 476 – 482, **2007**.
[29] Muralidhar L., Girija C.R., "Simple and practical procedure for Knoevenagel condensation under solvent-free conditions", *Journal of Saudi Chemical Society*, 18, 541-544, **2014**.
[30] Connolly D. J., Declan C., Timothy P. O. and Patrick J. G. "Synthesis of quinazolinones and quinazolines".*Tetrahedron*, 61, 10153 –10202, **2005**.
[31] Desai A. R., Roy R. U. and Desa K.R. "synthesis and antimicrobial screening of quinazolone containing novel heterocyclic schiff base and azetidinone by niementowski reaction". *E- J. Chem*., 2(2), 101 -108, **2005**.
[32] Ren Y. M. and Cai C.," knoevenagel condensation of aromatic aldehydes with active methylene compounds using a catalytic amount of iodine and k_2CO_3 at room temperature", *Synthetic Communications*, 37, 2209-2213, **2007**.
[33] Zabicky J. "the kinetics and mechanism of carbonyl-methylene condensation reactions. ". *J. Chem.Soc*., 0, 683-687, **1961.**
[34] Ismail M. M. F., Farrag A. M., Harras M. F., Ibrahim M. H., Mehany A. B. M. " Apoptosis: A target for anticancer therapy with novel cyanopyridines. ". *Bioorg. Chem.,* 94, 103481, **2020**.
[35] Kanhed A. A., Mehere A. P., Pandey K. R. and Mahapatra D. K., " 4-(2-chloroacetamido) Benzoic Acid Derivatives as Local Anesthetic Agents: Design, Synthesis, and Characterization", *Journal of Pharmaceutical and Biosciences*, 4(6), 35-44, **2016**.
[36] Acharyulu P.V., Dubey P. K., Reddy P.V. and Surech Th. "Synthesis of 2-(4-substitutedsulfonyl piperazin-1-yl-methyl)-3-aryl-quinazolin-4(3H)-one". *Ind., J., Chem*., 49(7), 923-928, **2010**.
[37] Al-Zaydia K. M., Al-Shamarya A. and Elnagdi M. H., "Studies with heteroaromatic amines. A new route to 2-azolylamino- 2-thiazolin-4-ones", *Journal of Chemical Research* , 408-411, **2006**.
[38] Puterová Z., Krutošíková A. and Végh D., "Gewald reaction: synthesis, properties and applications of substituted 2-aminothiophenes", *ARKIVOC*, *I*, 209-246, **2010**.
[39] Gouda M. A., "LiOH. H_2O as a catalyst for Knoevenagel and Gewald reactions", *J.Chem. Tech*., 12, 4, 31-35, **2010**.
[40] Abu-Hashem A. A., EL-Shehry M. F. and Badria F. A., "Design and synthesis of novel thiophene carbohydrazide, thienopyrazole and thienopyrimidine derivatives as antioxidant and antitumor agents" , *Acta Pharm* , 60, 311-323, **2010.**
[41] Kathiravan M. K., Shishoo C. J., Chitre T. S., Mahadik K. R. and Jain K. S., "Efficient Synthesis of Substituted 2-Amino-3- carbethoxythiophenes" , *Int. J. Rapid Communication of Syn. Org. Chem*., 37, 4273–4279, **2007**.
[42] Forero J. S. B., Carvalho E. M. d., Juniora J. J. and Flavia M. da. S., "A New Protocol For The Synthesis Of 2-AminoThiophens Through The Gewald Reaction In Solvent-Free Conditions ", *Heterocyclic Letts*., 1, 61-67, **2011**.

[43] Durgareddy G. A. N. K., Ravikumar R., Ravi S. and Adapa S. R., " A CaO catalyzed facile one pot synthesis of 2-aminothiophenes using Gewald reaction", *Der Pharma Chemica*, 5, 6, 294-298, **2013.**
[44] Wang, T., Huang, X., Liu, J., Li, B., Wu Chen, J.K., Zhu, W.L., Xu, X.Y., and Zeng, B.B.," An efficient one-pot synthesis of substituted 2-amino thiophenes via three-component Gewald reaction catalyzed by L-Proline", *Syn Lett,* 9, 1351-1354, **2010**.
[45] Ammar Y. A., El-Sharief A. M. S., Mohamed Y. A., Salem M. A., Al-Sehemi A. G. and El-Gaby S. A., " Cyano acetanilides Intermediates in Heterocyclic Synthesis. Part 1: A Facile Synthesis of Polysubstituted and Condensed Pyridones", *J. Chinese Chem. Society,* 51, 975-981**, 2004**.
[46] Koo J., Fish M. S., Walker G. N. and Blake J., "Working with Hazardous Chemicals ", *Org. Synth. Coll*. 4, 327, **1963**.
[47] Avanesyan A. A., Simonyan A. V., and Simonyan M. A. " Phosphorus Oxychloride In Organic Synthesis: Synthesis Of A-Benzoyl aminocinnamic Acids ", *pharmaceutical Chemistry Journal*, 39(7), 41-42, **2005.**
[48] Meerloo J. v., Kaspers G. J. L., and Cloos J., " Cell Sensitivity Assays: The MTT Assay", at: https: //www .researchgate .net/publication/51073437, **2011**.
[49] Gaber A. A., Bayoumi A. H., El-morsy A. M., Sherbiny F. F., Mehany A. B. M. and Eissa I. H.,." Design, synthesis and anticancer evaluation of 1H-pyrazolo[3,4-d] pyrimidine derivatives as potent EGFRWT and EGFRT790M inhibitors and apoptosis inducers", *Bioorganic Chemistry*, 80, 375–395**, 2018**.
[50] Ammar Y. A., El-Sharief A. M. S., Belal A., Abbas S. Y., Mohamed Y. A., Mehany A. B. M., Ragab A., " Design, synthesis, antiproliferative activity, molecular docking and cell cycle analysis of some novel (morpholinosulfonyl) isatins with potential EGFR inhibitory activity ", *European Journal of Medicinal Chemistry*, 156, 918–932, **2018**.
[51] Lakshmi P. J., Kumar B. V. S. S., Nayana R. S., M. Mohan S., Bolligarl R., Das S. K., Bhanu M. U., Kondapi A. K. and Ravikumar M., "Design, synthesis, and discovery of novel non-peptide inhibitor of Caspase-3 using ligand based and structure based virtual screening approach", *Bioorg. Med. Chem*., 17, 6040-6047, **2009**.
[52] Zilfou J. T. and Lowe S. W.," Tumor Suppressive Functions of p53; *Cold Spring Harb Perspect Biol*, **2009**.
[53] Antoine D., Olivier M. and Vincent Z., "SwissADME: a free web tool to evaluate pharmacokinetics, drug likeness and medicinal chemistry friendliness of small molecules", *Sci. Rep*. 7, 42717.
[54] Daniel F. V., Stephen R. J. Hung-Y. C., Brian R. S., Keith W. W. and Kenneth D. K.; "Molecular Properties That Influence the Oral Bioavailability of Drug Candidates", *J. Med. Chem*., 45, 2615-2623, **2002**.
[55] Marciane M. d. S., Marina C., Thiago S. D., Mary A. F., João E. d. C., Maria d. C. V. and Anelise S. N. F.," Synthesis, Antiproliferative Activity and Molecular Properties Predictions of Galloyl Derivatives", *Molecules*, 20, 5360-5373 , **2015.**
[56] Yuan H. Z., Michael H. A., Joelle L., Anne H., Chris N. L., Gordon B., Brad S. and Ian C.," Rate-Limited Steps of Human Oral Absorption and QSAR Studies", *Pharmacol. Res.*19, 1446-1457, **2002**.

Design and Synthesis of Novel Tranilast Analogs: Docking, Antiproliferative Evaluation and *In-silico* Screening of TGFβR1 Inhibitors

Magda M.F. Ismail[a]*, Heba S.A. El-Zahabi[a], Rabab S. Ibrahim[a], Ahmed B. M. Mehany[b]

- **PC-3 IC_{50}=1.1 µm**
- **HepG-2 IC_{50}=1.5 µm**
- **MCF-7 IC_{50}=2.6 µm**
- **TGFβR1 IC_{50}=0.087 µm**

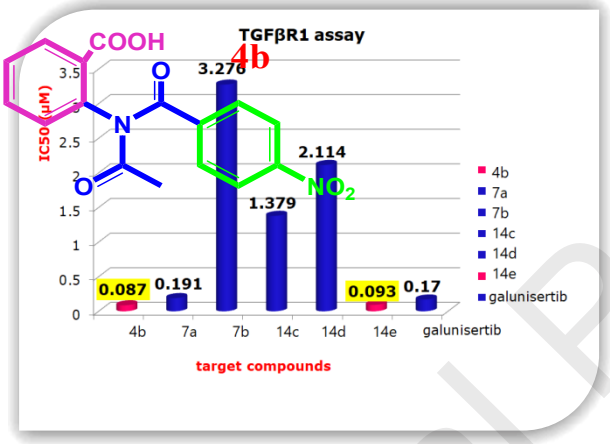

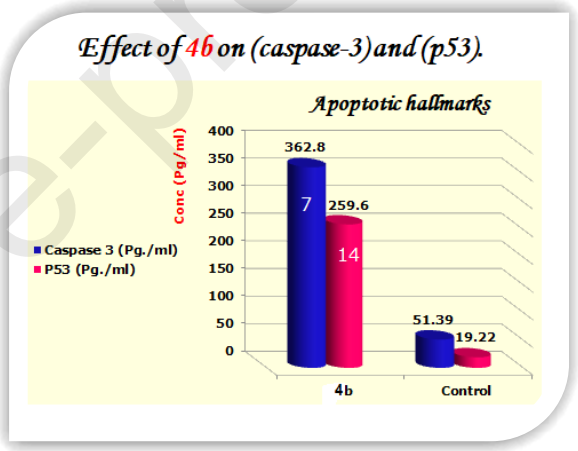

Research highlights

- Novel series of tranilast analogs is synthesized as potential selective anticancer on PC-3, HepG-2 and MCF-7 cell lines using 5-FU as reference drug.
- Twelve of the investigated compounds showed more potent cytotoxic agents than 5-FU, compound **4b** displayed amazing anticancer activity 5-7 times that of reference drug against all the tested cell lines.
- Target compounds **4b**, **7a** and **14e** were the most potent TGFβR1 inhibitors showing IC_{50}s in sub-micromolar range (IC_{50}'s 0.08, 0.09, and 0.19 µM).
- **4b** enhanced apoptosis and arrested G2/M phase of cell cycle. Besides, it induced apoptosis via the increase of both caspase-3 level and expression of p53 gene of PC-3 cell.
- *In silico* study revealed that all target compounds are in agreement with the parameters of Lipiniski's rule and Veber's violation.
- Molecular docking of the most potent hits, **4b** and **14e** elicited higher affinities to their respective binding site (TGFβR1) with good binding energies compared to ligand 460 and lead compound, tranilast.